



Bulletin of the Mineral Research and Exploration

<http://bulletin.mta.gov.tr>



Geological, mineralogical-petrographical and fluid inclusion characteristics of the Çatalçam (Soma-Manisa) Au-Pb-Zn-Cu mineralization

Ramazan SARI^{a*}, Şahset KÜÇÜKEFE^a, Gülcan BOZKAYA^b, Ömer BOZKAYA^b, Fatih BADEMLER^c, Zehra DEVECİ ARAL^c, Elif Dilek BAYRAKÇIOĞLU^c, Cahit DÖNMEZ^c and Serkan ÖZKÜMÜŞ^c

^aGeneral Directorate of Mineral Research and Exploration, Northwest Anatolia Regional Directorate, Balıkesir, Türkiye

^bPamukkale University, Faculty of Engineering, Department of Geological Engineering, Denizli, Türkiye

^cGeneral Directorate of Mineral Research and Exploration, Department of Mineral Research and Exploration, Ankara, Türkiye

Research Article

Keywords:

Northwestern Anatolia,
Lower Miocene
Magmatism, Porphyry-
Epithermal Au-Cu
Mineralization, Fluid
Inclusion.

ABSTRACT

The study area is located in the southeastern Biga Peninsula. As result of field, drilling and laboratory studies, diorite porphyry intruded to Lower Miocene and older units and contained Au, Pb, Zn and Cu anomalies, has been determined. Intersected potassic, propylitic, phyllic and argillic alteration zones were developed in the pluton and host rock. Veins-veinlets developed in the pluton and host rock, contain native gold, silver, pyrite, chalcopyrite, sphalerite and galena. They are composed of undulated quartz in the deeper levels, and massive quartz, calcite/dolomite and barite in the middle and upper levels. According to the fluid inclusion data from sphalerite, quartz and barite, temperature of ore-bearing fluids are in three groups (argillic:150-220°C, phyllic:250-350°C, potassic:>400°C). Fluid inclusions, including solid phases such as hematite, chalcopyrite and salt as well as liquid and gas phases, indicate that Çatalçam Au-Cu mineralization is intrusion-related system. Fluid inclusion data display temperature and salinity of the ore-bearing fluids in the early stage (porphyry) are high, whereas relatively lower in the late stage (epithermal). In conclusion, Çatalçam mineralization was developed in two different phases as porphyry Au-Cu and epithermal Zn-Pb-Cu-Au, which is the first porphyry gold deposit related to Miocene magmatic-hydrothermal system in the Biga porphyry belt.

Received Date: 18.10.2020

Accepted Date: 28.04.2021

1. Introduction

The world's copper needs are mostly provided by porphyry deposits. Ore deposits have been observed throughout the Alpine-Himalayan belt, as well as in Turkey, associated with collision and post-collision-related magmatism following the closure of the Neotethys Ocean (Richards, 2009, 2015; Hou et al., 2011; Lu et al., 2015; Chen et al., 2015; Li et al.,

2017; Kuşçu et al., 2019a, b; Tang et al., 2021 and inside references). The Western Anatolian Region and especially the Biga Peninsula, which is located within the Tethyan Eurasian Metallogenic Belt (Janković, 1997; Jingwen et al., 2014) or the Tethys Metallogenic Belt (Yiğit, 2012), is a very important region for active mineral exploration and operations as it hosts many epithermal and porphyry deposits (i.e., Yiğit, 2009, 2012; Kuşçu et al., 2019a, b; Oyman, 2019). The

Citation Info: Sari, R., Küçükefe, Ş., Bozkaya, G., Bozkaya, Ö., Bademler, F., Deveci Aral, Z., Bayrakçioğlu, E. D., Dönmez, C., Özkümüş, S. 2022. Geological, mineralogical-petrographical and fluid-inclusion characteristics of the Çatalçam (Soma-Manisa) Au-Pb-Zn-Cu mineralization. Bulletin of the Mineral Research and Exploration 167, 25-49.
<https://doi.org/10.19111/bulletinofmre.930094>

*Corresponding author: Ramazan SARI, rsaminta@hotmail.com

complex geological background of the Biga Peninsula makes it difficult to understand the magmatic and metallogenic evolution of the region. The calc-alkaline magmatism that occurred in the Cenozoic period between 52 and 18 Ma in the region, is an ore-bearing (fertile) phase such as its equivalent in the Tethys metallogenic belt (Richards, 2015; Kuşcu, 2019a).

Since the discovery of the Kışladağ porphyry Au deposit, the Western Anatolia region gained importance as a metallogenic belt for porphyry Au mineralization. Twenty-eight occurrences or deposits are known in the region and divided into three distinct belts defined as Biga, Tavşanlı and Afyon-Konya porphyry zones (Figure 1; Kuşcu et al., 2019a). The Muratdere porphyry Cu-Mo, Tepeoba porphyry Mo and Kışladağ porphyry Au deposits, which have been operated and are still being operation, are located in the Tavşanlı, Biga and Afyon-Konya porphyry belts, respectively. In addition to the Ağıdağı deposit discovered in the 1990s, the Halılağa (Etili, Çanakkale) and Karaayı (Kuşçayır, Çanakkale) porphyry deposits are newly discovered deposits (Kuşcu et al., 2019a, b). Gürcüler, Alaçam, Dikmen, Sarıçayır, Karapınar, Gelemiş, Topuk (Bursa), Tüfekçikonak (Kütahya), Tepeköy (Gökçeada) and Kocatarla

(Çanakkale), Eğmir (Edremit) are other examples of occurrences in Western Anatolia. These occurrences have been explored by field and geophysical methods together with drilling studies. But there is no detailed information could be found since they have not been publicly announced.

In Biga Peninsula, which is one of the lands where mining began in Anatolia, mineral exploration activities have been carried out intensively by the General Directorate of Mineral Research and Exploration since 2014 in order to find new potential resources, apart from the occurrences and deposits mentioned above. The Çatalçam mineralization, which is the subject of this study, is located in the southeast of the Biga Peninsula in Western Anatolia, near the Çatalçam Village, in the northwest of the Soma District of the Manisa Province. This mineralization is associated with a diorite porphyry body called Çatalçam Pluton (Sarı et al., 2018a, b), which is thought to belong to a magmatic phase not previously described in the literature. Çatalçam Pluton intruded to the Lower Triassic-Lower Miocene aged units, and its age is probably Middle or Upper Miocene. This unit is the firstly explored, economically important Miocene aged pluton located in the Biga porphyry belt

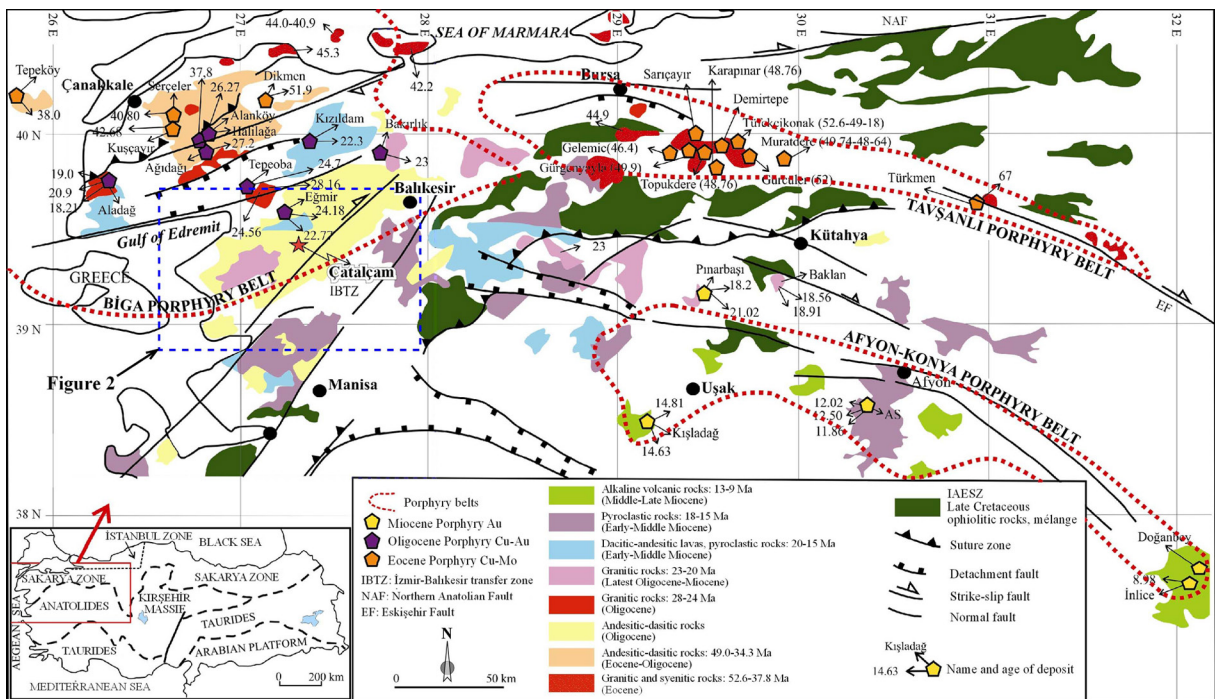


Figure 1- Distribution of Eocene-Miocene igneous rocks and porphyry mineral deposits in the Western Anatolia region (simplified from Kuşcu et al., 2019a) and the location of Çatalçam mineralization. The main tectonic units of Turkey were taken from Ketin, 1966, and Okay and Tüysüz, 1999.

in Western Anatolia and this exploration will bring a new perspective to mineral exploration studies.

In the study area, exploration on the surface with geological and geochemical methods and investigation with drilling studies are carried out. Fluid inclusion studies were carried out to determine formation conditions. Thin and polished section investigations were performed to determine mineralogical and petrographic features of host rock and ore samples. Alteration properties developed by hydrothermal fluids in host rock were examined. Within the scope of this paper, data from the mineralogical-petrographical investigation, alteration, and fluid inclusion studies were evaluated and the properties and formation conditions of the mineralization have been examined.

2. Material and Method

As a result of the field studies carried out since 2011, geology and alteration maps of the study area were prepared and orderly drill cores were carried out by drilling in different dips and directions beginning from the ore-bearing outcrops. Drilling core samples are divided into two equal parts with diamond cutting discs. One of these parts is used for chemical analysis, the other part is used for mineralogical-petrographic sampling and fluid inclusion studies. The remained core slices were held as replicate samples. The samples for mineralogical-petrographical and fluid inclusion analyses are firstly macroscopically examined to understand the relationship with host rocks and ore formations and then photographed.

Optical microscope investigations were carried out at the General Directorate of Mineral Research and Exploration Mineralogy-Petrography Unit and Pamukkale University Department of Geological Engineering using polarizing petrographic and reflected-light microscopes.

X-ray diffraction (XRD) method is used to determine the very small (submicroscopic) grain size components (e.g., clay minerals) and carbonate minerals. The samples used in XRD studies were first broken into 3-5 cm pieces with a hammer. Then, it was crushed into particles smaller than 5 mm in a jaw crusher and ground in a ring grinder for about 10-30 minutes, based on their hardness. After the powder material is prepared, samples are made for analysis by putting them into nylon bags and labeled. XRD

analyses were performed at Pamukkale University, Department of Geological Engineering, in GNR APD 2000 PRO brand X-ray diffractometer (Anode= Cu, $\lambda = 1.541871 \text{ \AA}$, filter = Ni, voltage = 40 kV, current = 30 mA, goniometer speed = $2^\circ/\text{min}$, shooting range, $2\theta = 5-45^\circ$). As a result of XRD analysis, the mineral components of the samples were defined and semi-quantitative percentages were calculated based on the mineral intensity factors determined by the external standard method (Yalçın and Bozkaya, 2002).

For fluid inclusion studies, two-sided polished sections were prepared at Pamukkale University, Department of Geological Engineering, Fluid Inclusion, and Ore Microscopy Laboratory. Micro thermometric examinations of fluid inclusion sections were performed by using LINKAM THMS-600 and TMS 92 type cooling and heating systems mounted on an Olympus Labophot-Pol type polarizing research microscope at the Fluid Inclusion and Ore Microscopy Laboratory in the same department. Initial melting (T_{FM}), last melting ($T_{m_{ICE}}$), homogenization of the samples (TH), and melting of salt crystals (T_{m-NaCl} , T_{m-KCl}) temperature measurements were carried out, and the accuracy in all measurements was stated as less than $\pm 0.5^\circ \text{C}$.

3. Geological Location and Lithology

The Biga Peninsula, which is the northwest end of the Anatolian plate, is located in the westernmost part of the Sakarya Zone. The region was formed as a mosaic by the amalgamation of continental parts with different geological backgrounds along the İzmir-Ankara-Erzincan Suture Belt with the closure of the Neotethys Ocean (Figure 1). The Anatolide-Tauride Belt of Gondwana is located in the south of the suture belt while the Sakarya Zone is located in the north (Figure 1). Most of the region consists of core complexes and outcrops of these core complexes that are associated with volcanic, sub-volcanic and plutonic rocks.

The pre-Paleogene core complex units in the region outcrop as the Menderes Massif and İzmir-Ankara Zone in the south and east, and the Sakarya Zone and the Rhodope-Strandja Massif in the north and west (Figure 2). Basement rocks of Sakarya Zone, as well as Kazdağ and Uludağ Massifs which are composed of high-grade metamorphic rocks (amphibolite-granulite facies), outcropped in the study area and surroundings

(Duru et al., 2012). Greenschist-blueschist facies metamorphic rocks of the Kalabak group tectonically overlie the Kazdağ Massif. Kalabak group is overlain by Late Carboniferous-Permian aged arkose and carbonate rocks and at the top Late Permian-Triassic Karakaya complex. These units are unconformably overlain by Late Triassic-Eocene aged units that form the cover of the Sakarya Zone.

The region representing the Biga Peninsula and its south underwent compressional deformation in the Late Cretaceous-Eocene and Oligo-Miocene periods, extensional in the Early-Middle Miocene, and strike-slip faults in the neotectonic period (Yılmaz et al., 2001; Duru et al., 2012). While the Eocene volcanic rocks, which form the volcanic units in the region, exhibit compositions varying from basalt to trachyte/dacite, Oligocene volcanic rocks are composed of andesite, trachyandesite, basaltic trachy-andesite, basaltic andesite and dacite (Genç et al., 2012). Early-Middle Miocene lavas exhibit the same composition as Oligocene, while Upper Miocene aged mafic lavas are represented by basalts.

The first magmatic phase in the region is the product of arc magmatism and occurred in the post-collisional Eocene period. The ages of the igneous rocks range from 45.3 ± 0.9 – 38.1 ± 1.8 Ma and vary from basalt to dacite (Altunkaynak and Genç, 2008).

Eocene granitoids intruded into the basement of the Sakarya Zone, and their sub-volcanic and volcanic equivalents are also observed in the region. The region became terrestrial in the Oligocene period and magmatic activity continued intensely. This phase, which is widespread in the whole region, shows the characteristics of mantle-derived arc magmatism that is contaminated in the crust (Yılmaz et al., 2001). Magmatic bodies that have volcanic and sub-volcanic equivalents generally outcrop NE-SW trending. Volcanics, which are the surface equivalents of plutonic rocks, are divided into different formations considering their lithological and geochronological features (Genç et al., 2012).

The Oligo-Miocene magmatic phase is a fertile phase. Igneous rocks of this age are the target for mineral exploration. The Hallaçlar volcanics, which crops out in large areas, is one of the important units especially for mineral exploration, and the unit is advanced argillized and intensely silicified zones from place to place. Hallaçlar volcanics is important since it contains exhalative Fe and high sulfide gold mineralizations.

In the Biga Peninsula and its southern side, intense volcanic activity is observed with the lacustrine sediments during the Lower-Middle Miocene period. Generally, volcanics that consist of andesite,

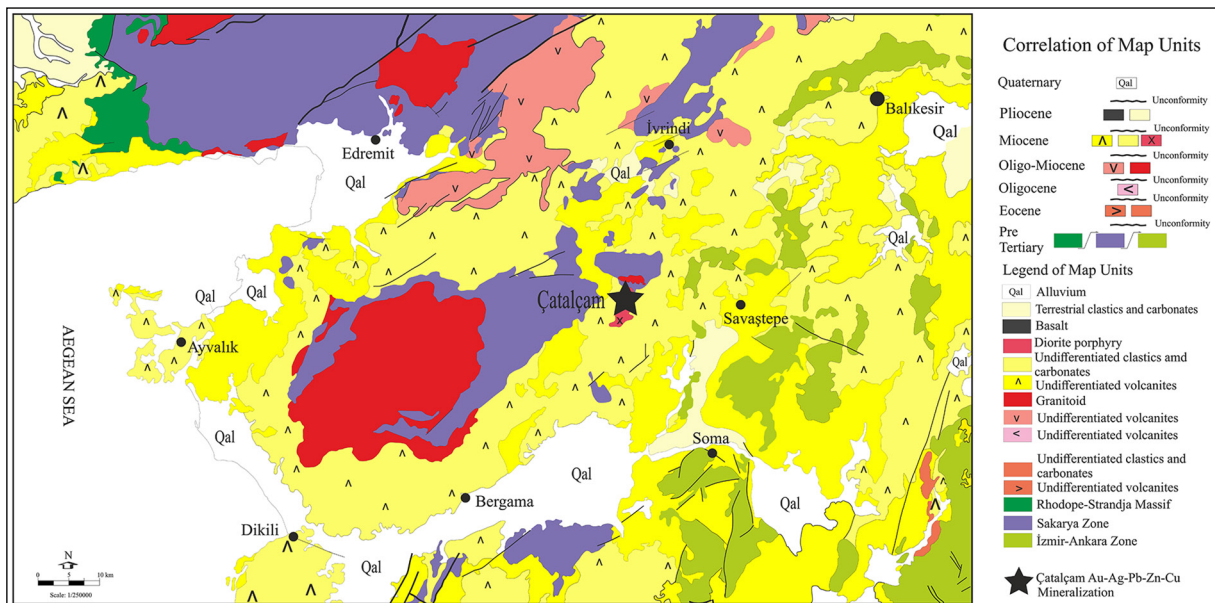


Figure 2- Regional geological map of the study area and its surroundings (Konak, 2002; Duru et al., 2012) and the location of Çatalçam mineralization are indicated.

trachyandesite, trachyte, latite, basaltic andesite type lava and pyroclastics are named by tip localities as Ezine Volcanics, Araplar Volcanics, Babakale Volcanics, Bademli Volcanics, Ortatepe Volcanics, Hazaldağ Volcanics, Şapçı Volcanics, and Yürekli Dacite (Genç et al., 2012). Şapçı volcanics (21.2±0.9 Ma) consists of white thick acidic tuffs that are partly ignimbrite at the bottom, followed by acidic lava and pyroclastics, and successively going upward with andesitic, basaltic andesitic lavas and pyroclastics, which form at the last stages of volcanism. Yürekli dacite consists of lava and pyroclastics with acidic components and is observed intercalated with lacustrine sediments. The Yuntdağ volcanite consists of andesitic lava and pyroclastics. These units are the Hüseyinfakı Volcanics and Arıklı İğnimbrite, which consists of basalt and trachyandesitic lava and pyroclastics; with pumice from place to place and it is accompanied by Ayvacık Volcanics, Babadere Dacite, Işıkeli Rhyolite, and Çamkabalak İğnimbrite, which

starts with ignimbritic tuffs and consists predominantly of basaltic andesite and andesitic pyroclastics (Genç et al., 2012). The last magmatic phase in the region was formed in the Late Miocene (11.0±0.4–8.32±0.19 Ma) and is dominant in terms of magmatic activity with alkaline composition, in which mafic rocks are formed. In the study area and in its vicinity where Çatalçam mineralization is located; the Triassic aged Karakaya Complex and Miocene aged magmatic activity products (both volcanic and plutonic rocks) crop out widespread in the region (Figure 3).

3.1. Karakaya Complex

The Karakaya Complex, which crops out in a narrow area in the northern part of the study area (Figure 3); is generally composed of grey, brown sandstone, metasandstone, shale, mudstone, metaconglomerate, basic volcanics and Carboniferous and Permian limestone blocks of different sizes (Duru et

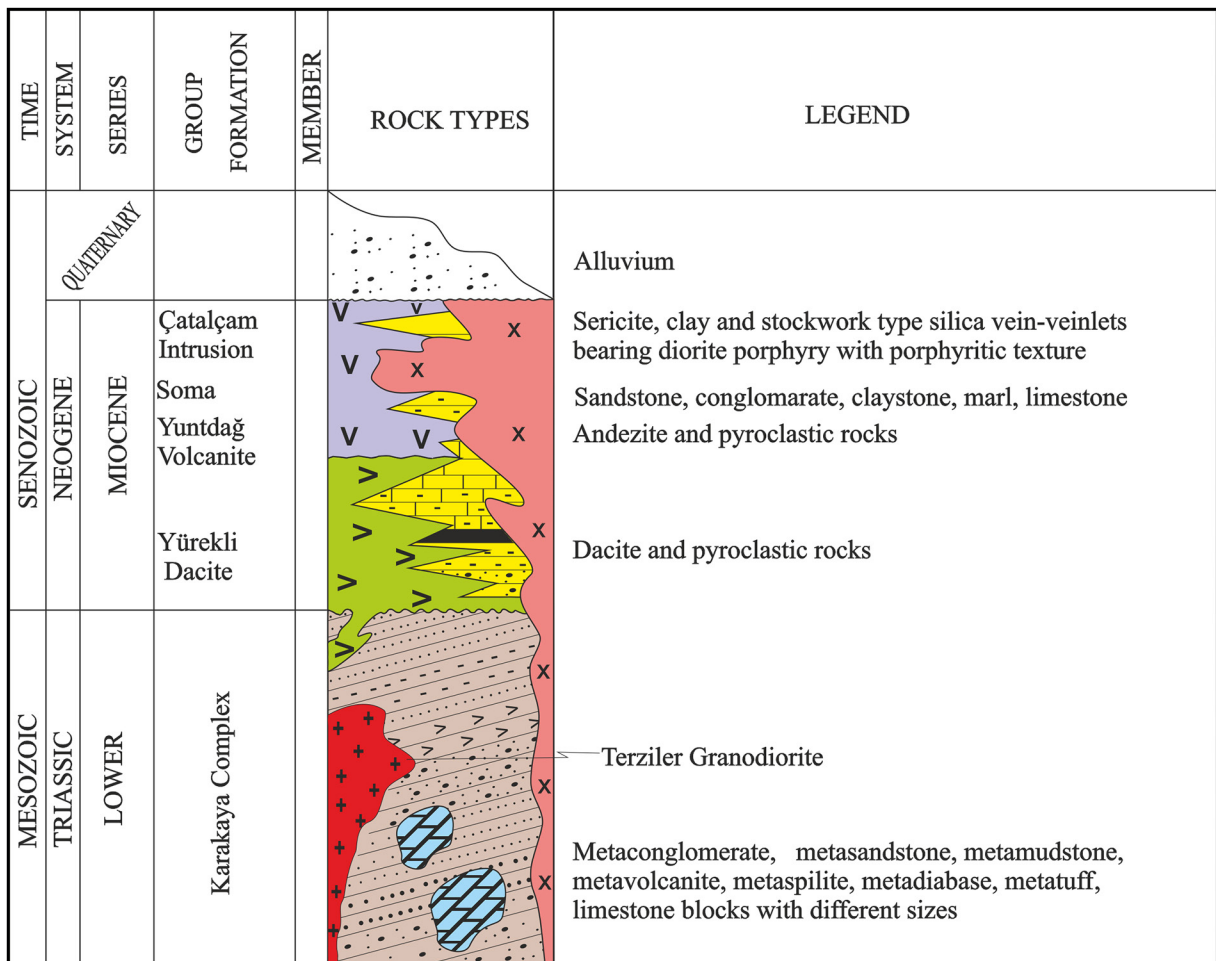


Figure 3- Stratigraphic section of the study area and its surroundings (Sarı et al., 2018a, b).

al., 2012). The lithologies in the unit, which do not show a regular sequence, are located in a lateral and vertical transitional and/or blocky. The unit has been affected heterogeneously by tectonic deformation. While primary sedimentary features are well preserved in some regions, blocks and low-grade metamorphism effects are observed in some locations that have been heavily affected by tectonic deformation (Tetiker et al., 2015).

3.2. Terziler Granodiorite

Terziler Granodiorite is outcropped in the north of the study area and intruded to the clastic and metavolcanic units of the Karakaya Complex (Figure 3 and Figure 4). It contains grey, dark grey, and greenish colored, hypidiomorphic granular texture, orthoclase, plagioclase, quartz, hornblende, biotite, and opaque minerals, as well as secondary sphene, zircon, and apatite (Ercan et al., 1984). Amphibole and biotite minerals are locally chloridized and disseminated pyrite+chalcopyrite are observed in the unit. Cu-Pb-Zn-Fe mineralizations are observed due to intrusion within the contact metamorphic zone developed at the contacts of Karakaya Complex and Terziler granodiorite.

3.3. Yürekli Dacite

The unit consists of gray, white-colored lava and pyroclastic rock fragments that are in acidic composition and rich in quartz and biotite minerals in hand specimen (Akyürek and Soysal, 1978). Yürekli Dacite is observed in the west of the study area and also outcrops in wide-area (Figure 4). The unit has calc-alkaline and post-collisional volcanic character, and it is stated that the main magma source forms an enriched lithospheric mantle (Saatci and Aslan, 2018). The unit spreads alternately with lacustrine sediments from place to place and contains silicified trees and perlite formations.

The lavas that have hypocrySTALLINE porphyritic texture contain plagioclase, quartz, alkali feldspar, biotite, apatite, opaque minerals, and are defined as dacite and rhyolite. The rock consists of medium-grained, euhedral-subhedral feldspar, and anhedral quartz minerals together with euhedral-subhedral biotite minerals. Plagioclase minerals are in the albite-andesine composition according to anorthite content varying between 8-44%. Polysynthetic

twinning and zoning are observed in some of the plagioclase minerals. A small amount of opacification has occurred in the biotites. The matrix consists of devitrified volcanic glass and feldspar microliths and secondary minerals. The unit stratigraphically overlies the Hallaçlar volcanics and its age is Early Miocene (19.8 ± 0.3 ; 19.5 ± 0.1 ; 20.3 ± 0.6 Ma; Benda et al., 1974; Krushensky, 1976; Genç et al., 2012; Figure 3).

3.4. Yuntdağ Volcanics

Yuntdağ volcanics (Akyürek and Soysal, 1978) consists of calc-alkaline andesite, basaltic andesite, trachy-andesite lavas, and pyroclastic rocks. The unit crops out in the north of the study area with feldspar phenocrysts and porphyritic texture. The feldspar and mafic minerals of the unit, which are altered due to the Early Miocene diorite porphyry intrusion, are sericitized and chloritized. In the study area, disseminated galena+sphalerite+chalcopyrite, barite+quartz+calcite+dolomite vein-veinlets are also observed within the unit.

In the study carried out in the Yuntdağı volcanics located in the İzmir - Balıkesir Transfer Zone, it was stated that the region had undergone deformation since the Early Miocene (Karaoğlu, 2014). Radiometric age studies give ages in the range of 21.5–14.0 Ma (Borsi et al., 1972; Ercan et al., 1996; Figures 3 and 4).

3.5. Soma Formation

The Soma formation is a unit that is deposited in the Soma Basin, starts with Lower-Middle Miocene aged lacustrine and fan-delta deposits and continues with fluvial and shallow lake sediments that contain coal beds at an economic level (Nebert, 1978; Akyürek and Soysal, 1983; Dönmez et al., 1998; İnci, 1998, 2002). The Soma formation outcrops in the north, west, and southeast of the study area (Figure 4). It is generally white, yellow, gray, clayey limestone, clay, marl, siltstone, tuffite, sandstone, and conglomerate intercalated, and has occasionally economical lignite level. As a result of the drilling studies carried out by MTA, it was determined that the Soma formation was subjected to contact metamorphism and transformed into hornfels due to the Çatalçam Pluton (Figure 5). Within the siliceous and greenish-gray colored hornfels zone, disseminated pyrite and chalcopyrite zones, stockwork, locally disseminated pyrite±chalcopyrite quartz, and locally

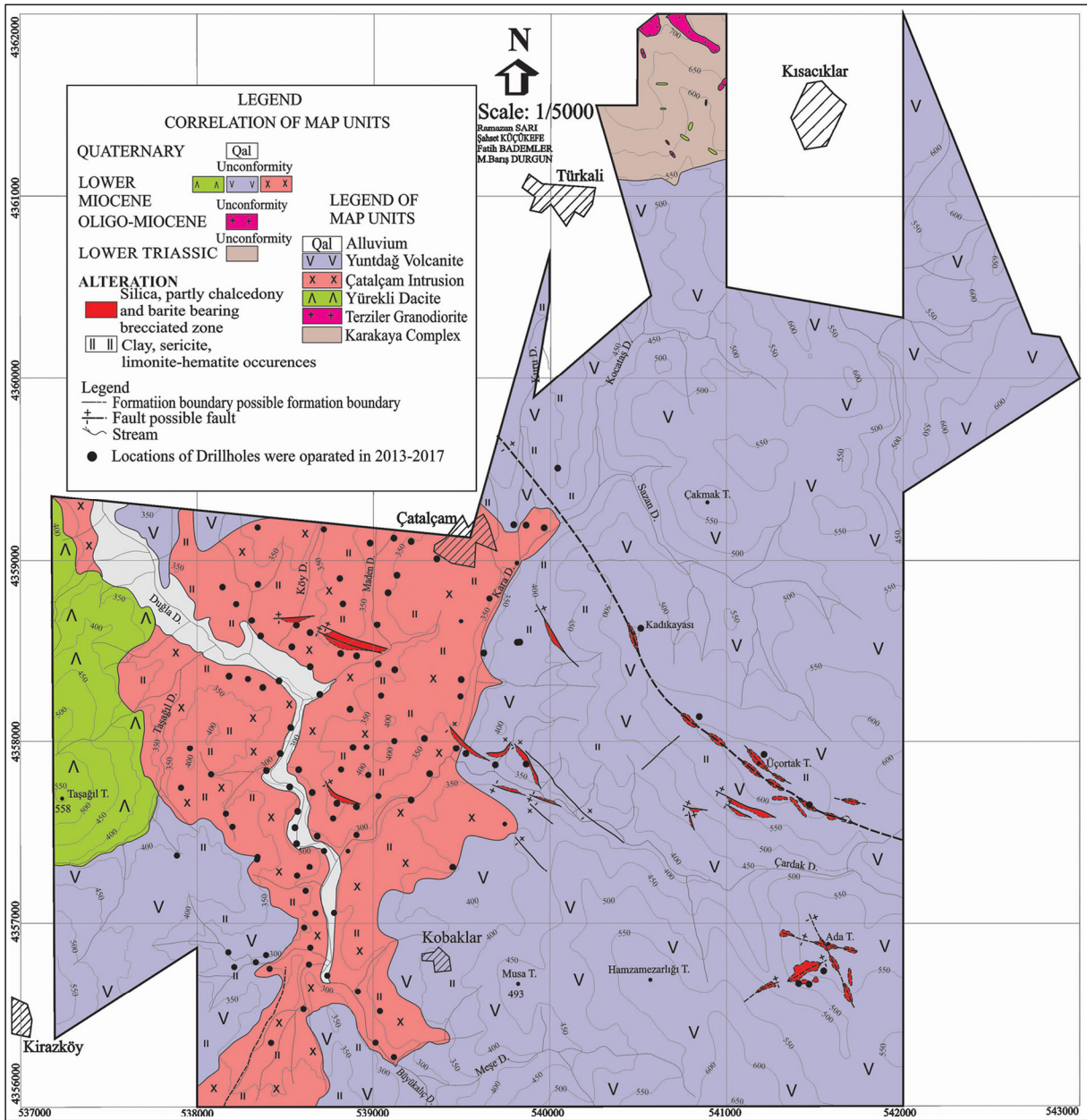


Figure 4- Geological map of the study area (Sarı et al., 2018a, b).

disseminated galena+sphalerite+chalcopryrite barite+quartz+calcite+dolomite veins/veinlets are observed. The lignite-bearing levels are anthracite due to contact metamorphism.

3.6. Çatalçam Pluton

The Çatalçam Pluton is firstly mapped and defined in the vicinity of Çatalçam as part of the polymetallic mineral exploration project carried out on the Biga Peninsula and its south by the team of the MTA Northwest Anatolia Regional Directorate.

The unit is in diorite-porphyry composition and has intruded very close to the surface and is emplaced at very shallow depths. The porphyritic textured rock is macroscopically composed of coarse plagioclase crystals and partially smaller amphibole and biotite crystals and a fine plagioclase microcrystalline matrix (Figure 6). As seen in Figure 6, it is rarely seen fresh, mostly feldspar phenocrysts are sericitized, partly argillized, and mafic minerals are pyritized, locally chloritized, and magnetized. The porphyritic texture is also observed microscopically and it is

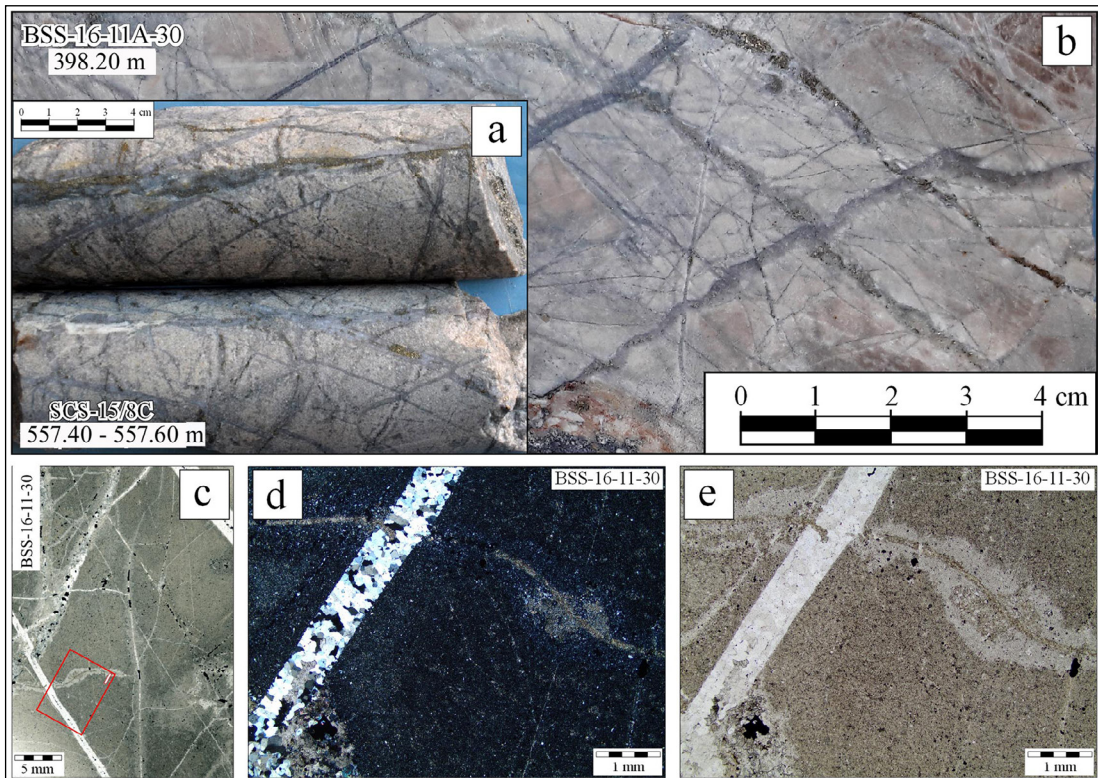


Figure 5- a), b) Drilling cores of the extremely silicified sandstone and claystone sample belonging to the Soma formation, which was transformed into hornfels by Çatalçam Pluton and containing ore-bearing quartz and calcite veins-veinlets, c) images of thin-section scanning, d) crossed-polarized light, and e) plane light.

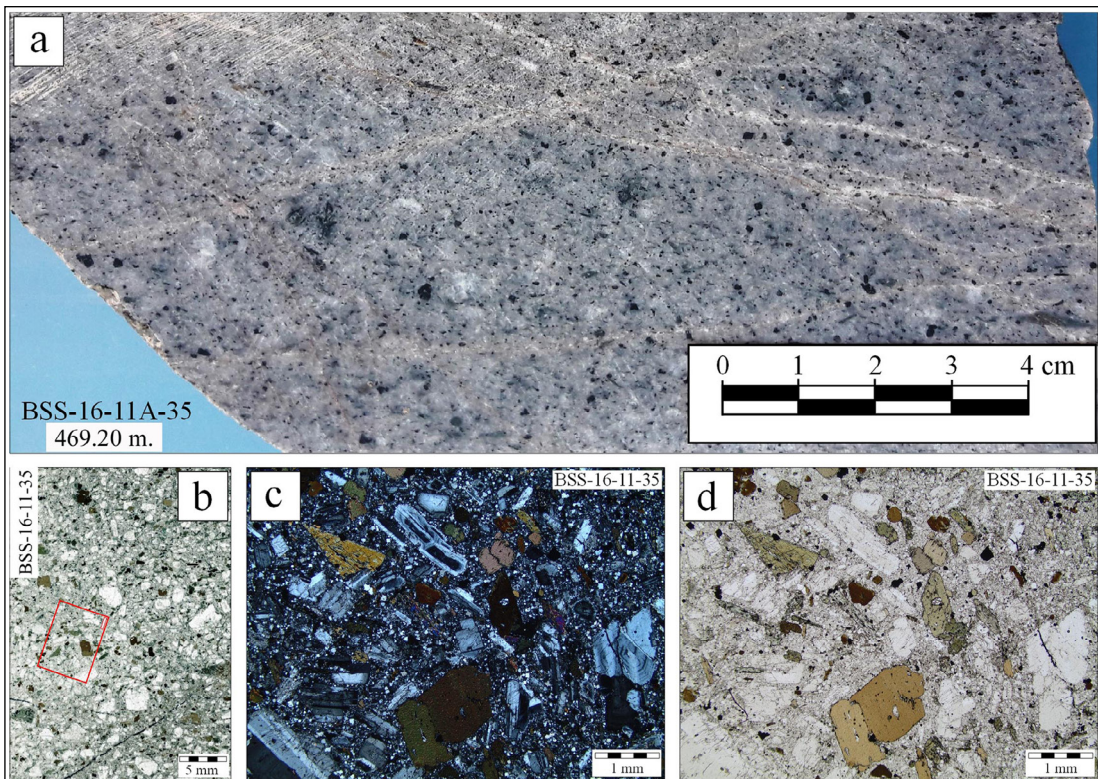


Figure 6- A fresh diorite porphyry sample taken from the drill core of the Çatalçam Pluton; a) drill core, b) images of thin-section scanning, c) cross-polarized light, and d) plane light.

defined as diorite porphyry with porphyritic texture with plagioclase, biotite, and amphibole phenocrysts (Figure 6). Plagioclases have platy and tabular prismatic shape. Amphiboles are mostly subhedral rod-like prismatic shaped, while biotites are mostly euhedral-subhedral foliate-plate-like shaped (Figure 6b, e and f). Biotite is observed as fine-grained hydrothermal biotite in clusters and vein-veinlets from place to place. The matrix consists of holocrystalline, fine-grained intergrown feldspar and probable quartz crystals. Apatite and zircon are determined as secondary minerals. Considering its microscopic features; it is defined as diorite porphyry with porphyritic texture with plagioclase, biotite and amphibole phenocrysts (Figure 6).

Au-Pb-Zn-Cu mineralization developed as quartz veins/veinlets in the diorite porphyry body. At the contact of the sedimentary rocks which the diorite porphyry intrudes, no primary rock texture is observed, and hornfels zone containing pyrite, galena, sphalerite, and chalcopyrite has developed as disseminated veins and veinlets (Figure 5). Veins and veinlets are filled with quartz and barite + calcite. The radiometric age of the unit has not been determined yet, but the intrusion is thought to have formed in the Early Miocene or later period, as it cuts the Early Miocene aged Soma formation and the same-aged Yürekli dacite and Yuntdağ volcanics.

4. Alteration

In the light of the information obtained mainly from field observations and partly from mineralogical-petrographic studies, it has been determined that potassic, propylitic, phyllic, and argillic alteration zones have developed in the study area and they are generally intersected and telescoping (Figure 7). Regarding mineralization; propylitic zone that contains epidote, chlorite, calcite, and limonite-hematite with quartz veins, pyrite and calcite, and/or dolomite veins/veinlets from place to place without ore minerals are observed in the outermost part (Figure 7). In the inner parts, intense clayey (kaolinite, interbedded illite-smectite, and illite), quartz with pyrite±chalcopyrite and disseminated galena + sphalerite + barite with chalcopyrite + quartz + calcite + dolomite vein-veinlet argillic zone is observed (Figure 7). Within this zone, N60E and E-W direction, brecciated textured, 0.2-5 m thick, ore veins-veinlets are observed. In the argillic zone,

intense sericite, partly clayey, dark gray disseminated pyrite±chalcopyrite quartz and galena + sphalerite + chalcopyrite barite + quartz + calcite + dolomite vein-veinlet and disseminated pyrite phyllic zone have developed (Figure 7). In the inner parts of the diorite porphyry, the potassic zone is observed. This potassic zone cannot be observed on the surface but can only be determined in drilling studies. This zone is gray-colored and consists of minor sericite and chlorite-bearing, partly epidote, partly magnetite vein-veinlet, partly disseminated pyrite±chalcopyrite, undulation quartz, disseminated galena+sphalerite±chalcopyrite-bearing barite+quartz+calcite+dolomite vein-veinlets, and hydrothermal biotite accumulations from place to place (Figure 7). Vein-veinlets developed in the diorite porphyry bodies have turned grey on the surface due to atmospheric conditions (Figure 8). In some parts of the study area, it is observed in yellowish-colored limonite and hematite due to pyrite alteration.

In addition to the alteration observed on the surface, intense alteration and locally ore-bearing quartz vein-veinlets were observed in the drill cores, both in the diorite porphyry body causing alteration and in the hornfels developed from the Soma formation due to intrusion. Besides the degree of alteration in diorite porphyry, especially the shape of veins and veinlets (solid or corrugated) and mineral composition (quartz, calcite, dolomite, barite) from the deep levels with potassic and phyllic alterations to the surface levels where the argillic alteration is intense, there is significant differences are observed. At deep levels (>400 m) representing the porphyry stage, gray-colored quartz fillings with corrugated vein-veinlets of various sizes, reaching 2 cm in thickness, are characteristically observed (Figure 9 and 10). The plagioclase phenocrysts are sericitized mostly and completely in places, sericite and fine-grained biotite crystals developed in the matrix due to alteration representing the potassic and phyllic zone. Dark-colored minerals (hornblende and biotite) are completely opaque (magnetitized) or chloritized. In the specimens at shallow depths (<75 m) representing the epithermal stage, vein-veinlets contain a smooth/uniform appearance and are filled with white quartz, calcite, and barite that reach 5 cm thickness (Figure 11 and 12). According to the textural relationship of the minerals filling vein-veinlets, it was determined that quartz formed at the first stage, then calcite and barite formed at the last stage. Sericitization

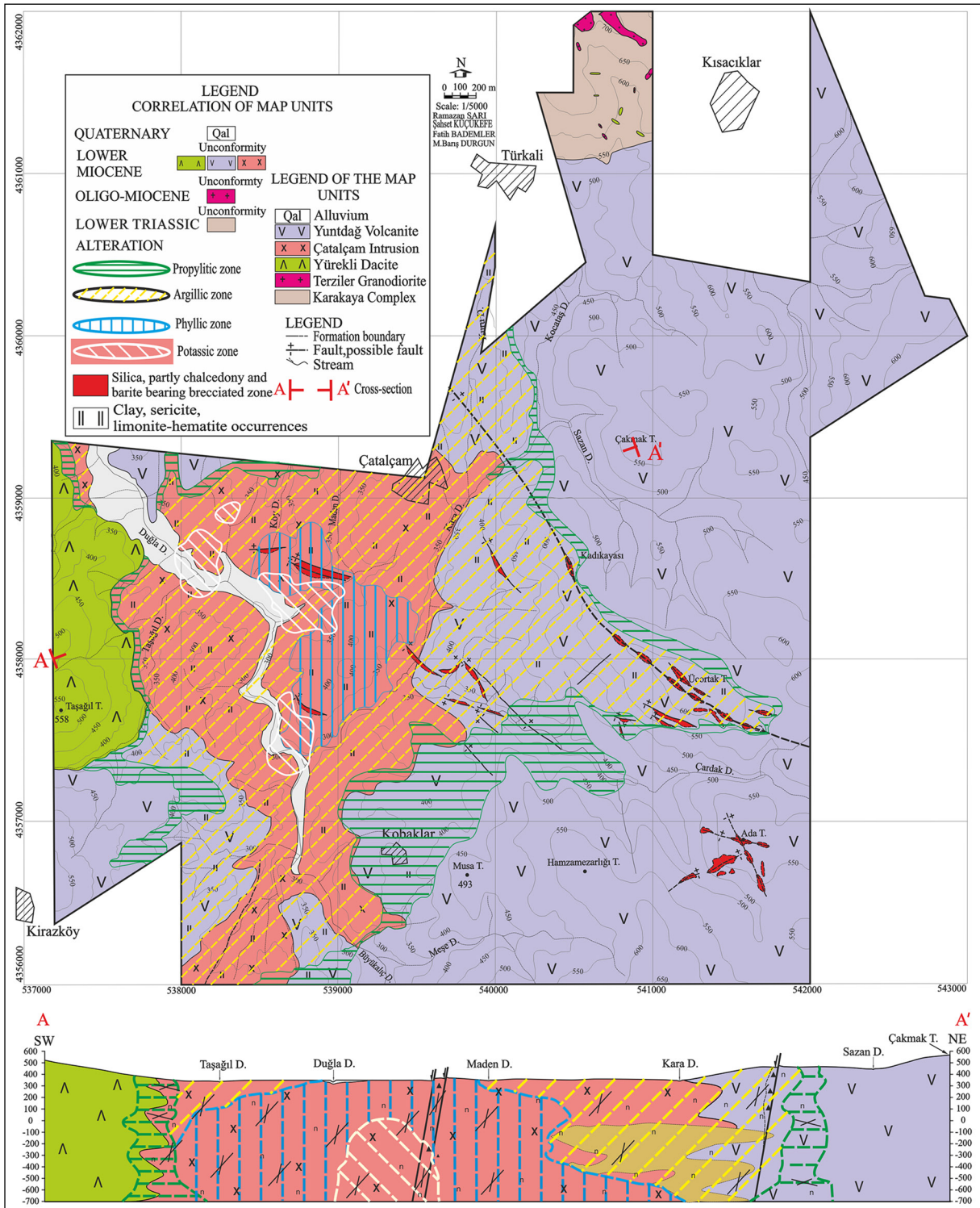


Figure 7- Alteration map and cross-section of the study area (Sarı et al., 2018a, b).

and argillization (kaolinization) are observed in the plagioclase and matrix in the samples representing the argillic zone, but fine-grained biotite formations are not observed. In order to determine the textural and mineralogical distributions of the alteration zones in

the vertical direction; optical microscopic and whole-rock X-ray diffraction (XRD) studies were carried out on altered samples representing different depths from BSS-16-11A drill cores (Figure 13). According to the data obtained, carbonate minerals are represented by



Figure 8- Field images from the Çatalçam Pluton with intense hydrothermal alteration and stockwork veins (qz: quartz, cal: calcite, bt: barite).

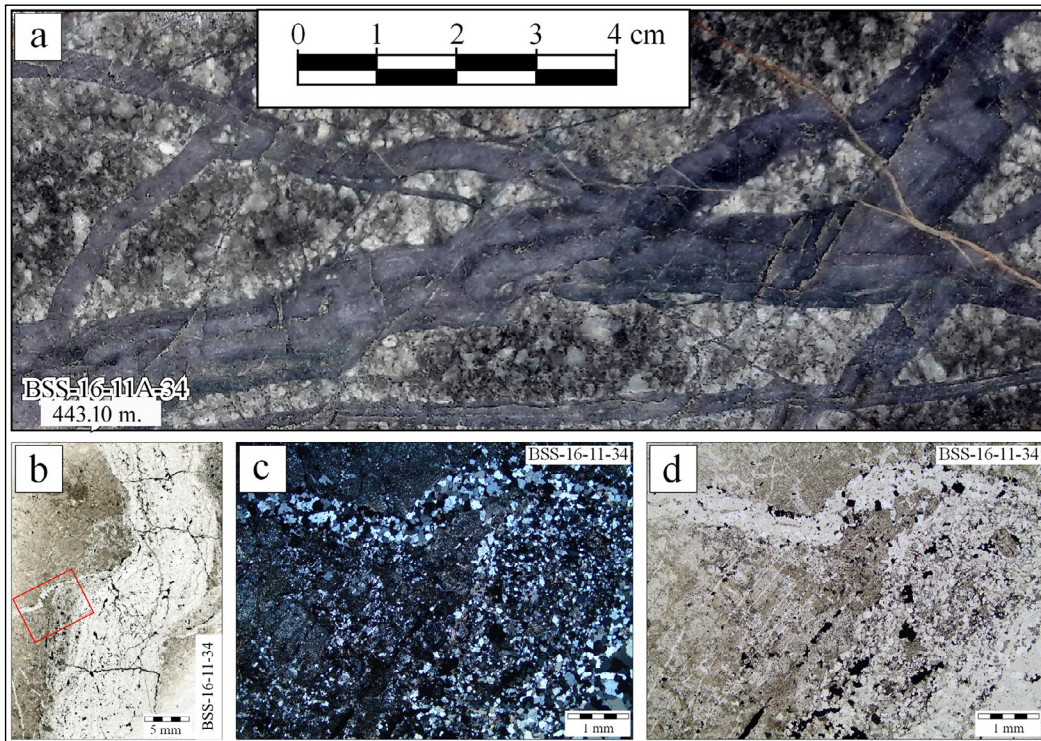


Figure 9- Images of; a) drill core, b) thin-section scanning, c) cross-polarized light, and d) plane light of undulated gray stockwork quartz vein-veinlets in altered diorite porphyry sample (BSS-16-11A-34) belonging to Çatalçam Pluton.

calcite in the near-surface sections (between 0-120 m) and by dolomite in the deeper level (between 200-350 m). Hydrothermal alteration product quartz and primary magmatic plagioclase constitute the main components of the samples. In addition to quartz, the barite-bearing samples representing the epithermal phase are accompanied by calcite at the upper levels and dolomite at the lower levels. Pyrites are observed in small amounts (usually 10% or less) at all levels.

Biotite is the product of potassic alteration and is determined by macroscopic and petrographic data. Biotites are formed at 300 m and deeper levels and accompanied by small amounts of chlorite and locally illite/muscovite. Illites (sericite as microscopically) are observed at almost all levels (phyllitic zone) and their amount increases slightly towards the upper levels. Kaolinite forms in small amounts (<20%) increasing towards the upper levels and it is observed at all levels but does not form pure clay mineral component.

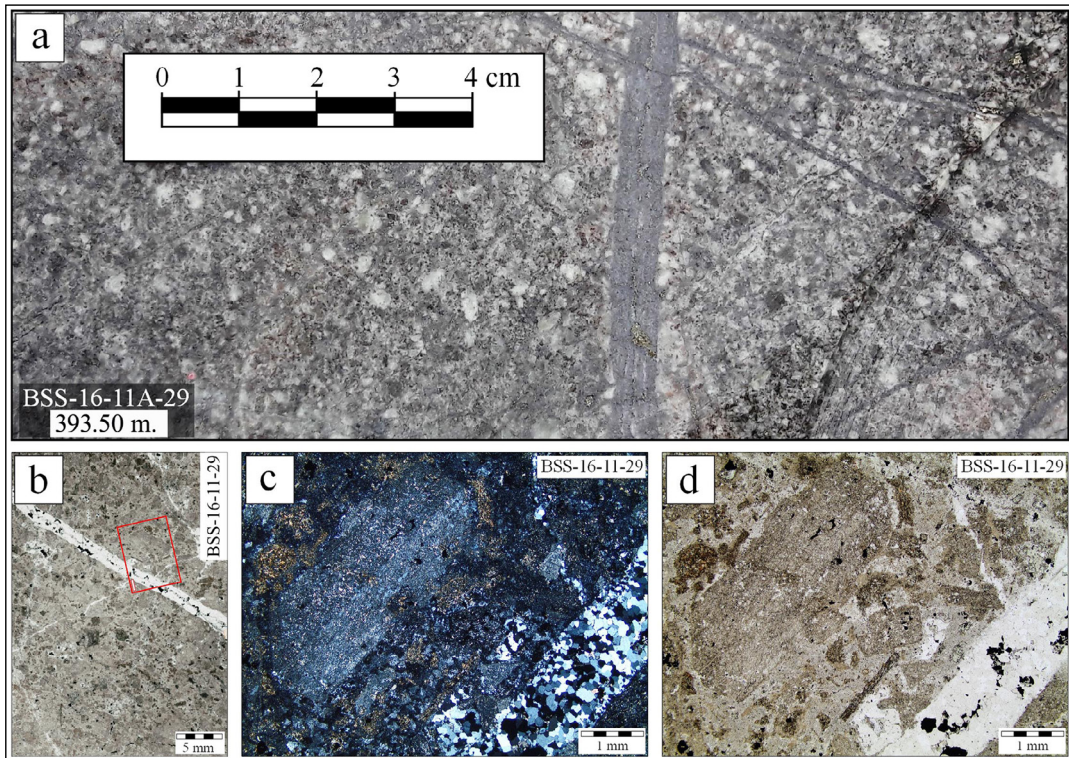


Figure 10- Images of; a) drill core, b) thin-section scanning, c) cross-polarized light, and d) plane light of sericitized plagioclases and ore-bearing gray-colored quartz vein-veinlets within the silicified, sericitized, and fine-grained biotite-containing matrix in the altered diorite porphyry sample (BSS-16-11A-29) belonging to the Çatalçam Pluton.

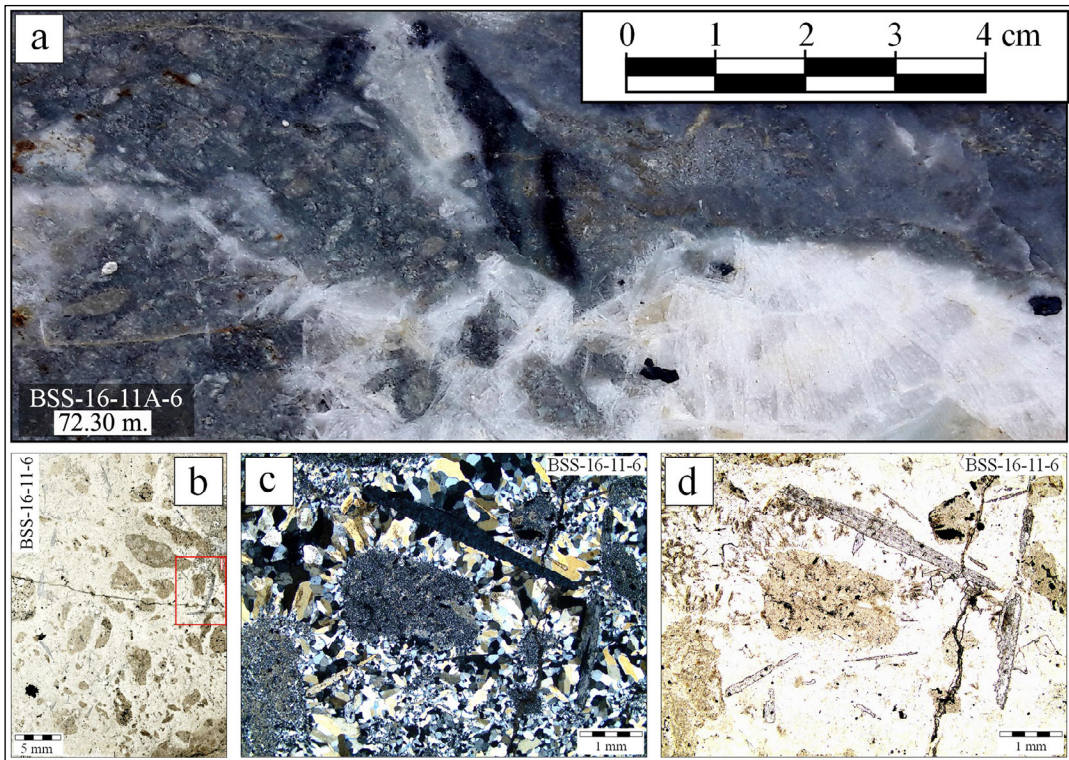


Figure 11- Images of; a) drill core, b) thin-section scanning, c) cross-polarized light, and d) plane light of fine and coarse-grained, partly chalcedonic quartz vein cut by the bar-shaped prismatic barite-bearing uniform (massive) white colored vein of altered diorite porphyry sample (BSS-16-11A-6) belonging to the Çatalçam Pluton.

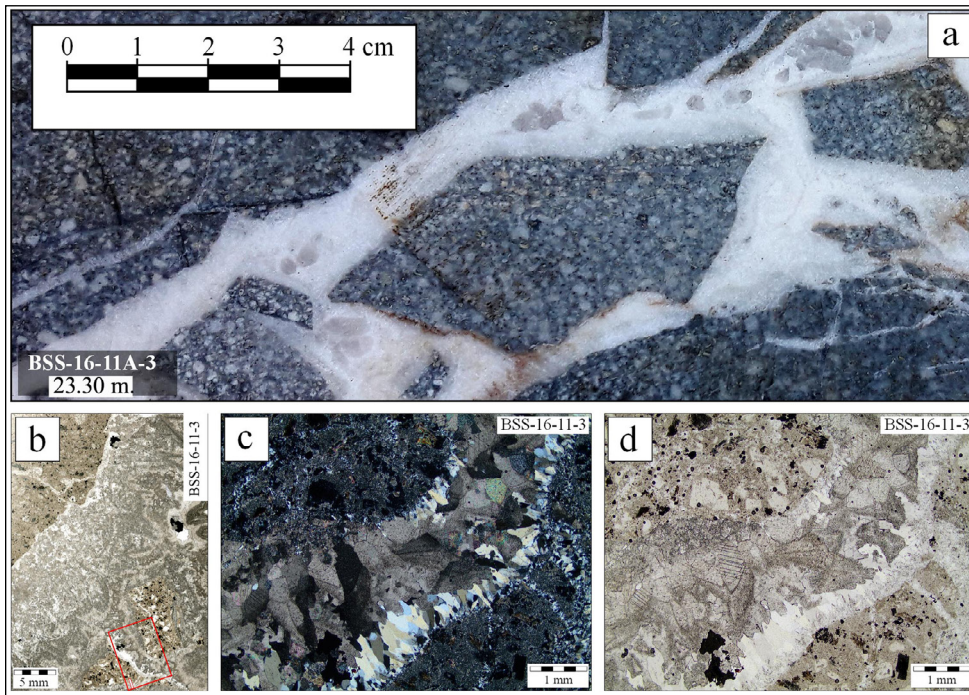


Figure 12- Images of; a) drill core, b) thin-section scanning, c) cross-polarized light, and d) plane light of the altered diorite porphyry sample (BSS-16-11A-3) belonging to the Çatalçam Pluton, the uniform (massive) white vein containing quartz and calcite filling the altered diorite porphyry breccia.

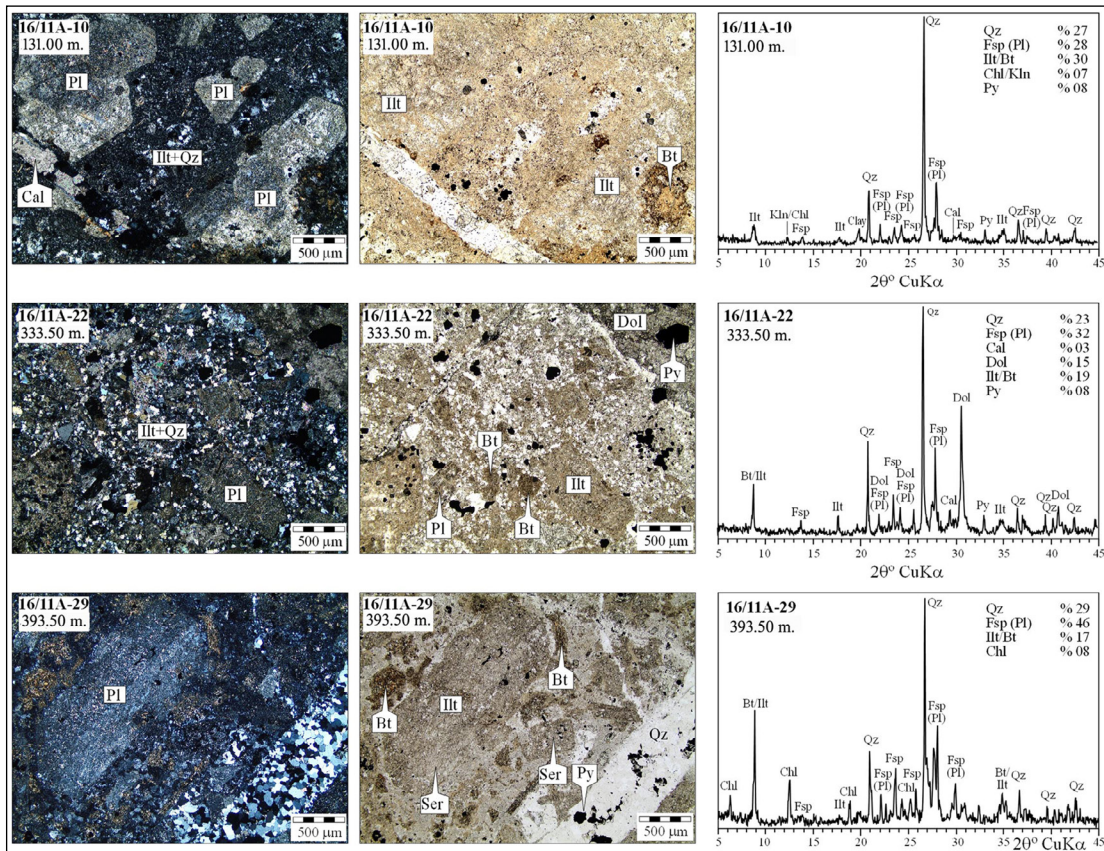


Figure 13- Distribution of alteration-related mineralogical compositions of the altered diorite porphyry samples belonging to the Çatalçam Pluton according to depths (Qz: quartz, Fsp: feldspar, Pl: plagioclase, Bt: biotite, Ilt: illite, Ser: sericite, Chl: chlorite, Kln: kaolinite, Cal: calcite, Dol: dolomite, Py: pyrite).

5. Mineralization

As a result of detailed geological and geochemical studies in the field, As, Sb, Ag, Pb, Zn, Cu, Au, and Mo anomalies were determined (Sarı et al., 2018a, b). Cu-Zn-Au-Mo and Sb-As-Ag-Pb-Zn-Cu-Au anomaly groups overlap in the same area, and the Lower Miocene aged Yürekli dacite on the surface spatially overlaps with the alteration areas developed due to the Çatalçam Pluton.

As a result of the surface and drilling studies; In an area of approximately 4 km², economically exploitable porphyry type Au mineralization with an average grade of 0.2-1 gr/ton was determined. This mineralization creates an economically exploitable resource; It is accompanied by Ag with an average grade of 8 ppm and Pb+Zn with an average grade of 1.8-2%.

From the surface and drilling studies, 4 different types of mineralization have been determined in the study area, and their important features are mentioned below.

Type 1 mineralization: Hornfels zones that formed by the intrusion into the Early Miocene Soma Formation of diorite porphyry that is the source of mineralization in the field that does not outcrop but was cut in drilling cores. These hornfels zones contain quartz densely and partly brecciated, it includes disseminated and fillings pyrite+chalcopyrite+galena+sphalerite+gold mineralization in vein-veinlets (Figure 5).

Type 2 mineralization: Related with the Çatalçam Pluton; Within the volcanics (andesite) white-colored, sericitized feldspars, chloritized, pyritized mafic minerals, clayey, disseminated pyrite-bearing altered zones with abundantly and stockwork white galena+sphalerite+chalcopyrite and epigenetic Au-Pb-Zn barite+quartzite vein calcite+ dolomite vein-veinlets can be seen (Figure 14).

Type 3 mineralization: It contains pyrite+chalcopyrite+galena+gold+fahlerz group minerals and rarely molybdenite mineralization, which are gray-dark gray-colored, locally stockwork-brecciated quartz vein-veinlets within the Çatalçam Pluton (Figure 15).

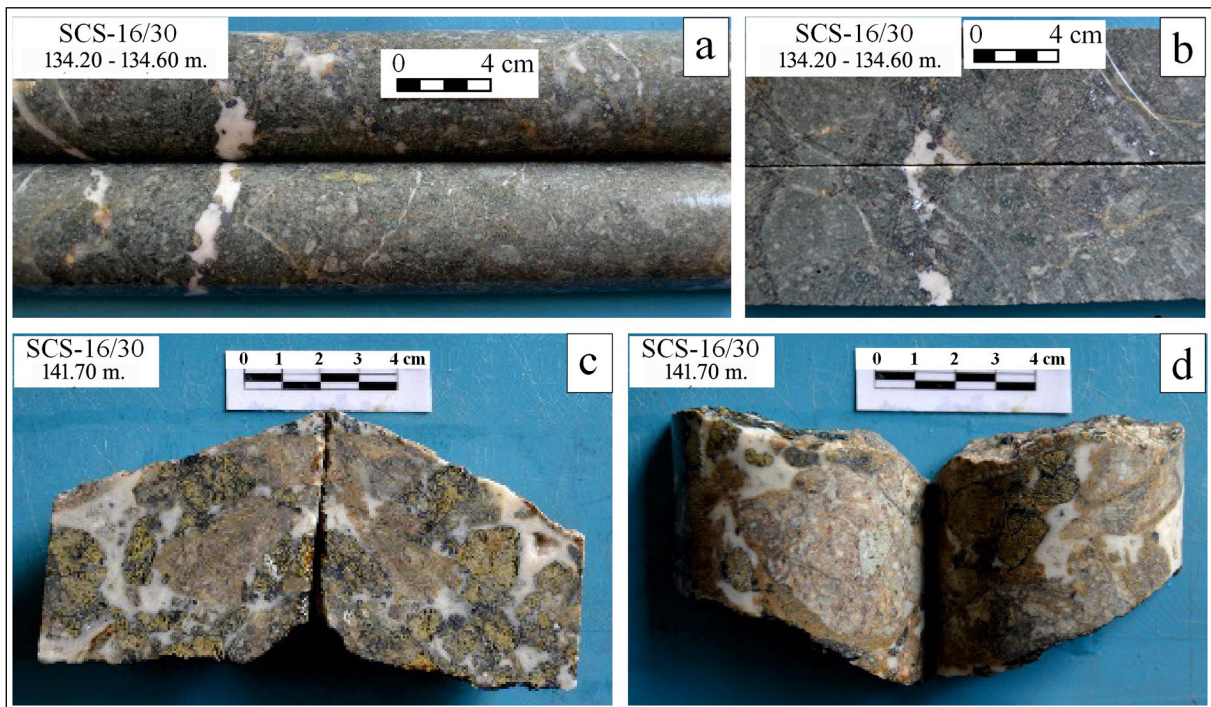


Figure 14- The disseminated galena+sphalerite+chalcopyrite-bearing barite+quartz+calcite veins-veinlets determined in the drilling studies in altered andesites; a), b) disseminated galena+sphalerite+chalcopyrite mineralization in barite+quartz+calcite+dolomite veins, c), d) densely disseminated galena+sphalerite+chalcopyrite mineralization within barite+quartz+calcite+dolomite vein-veinlets.

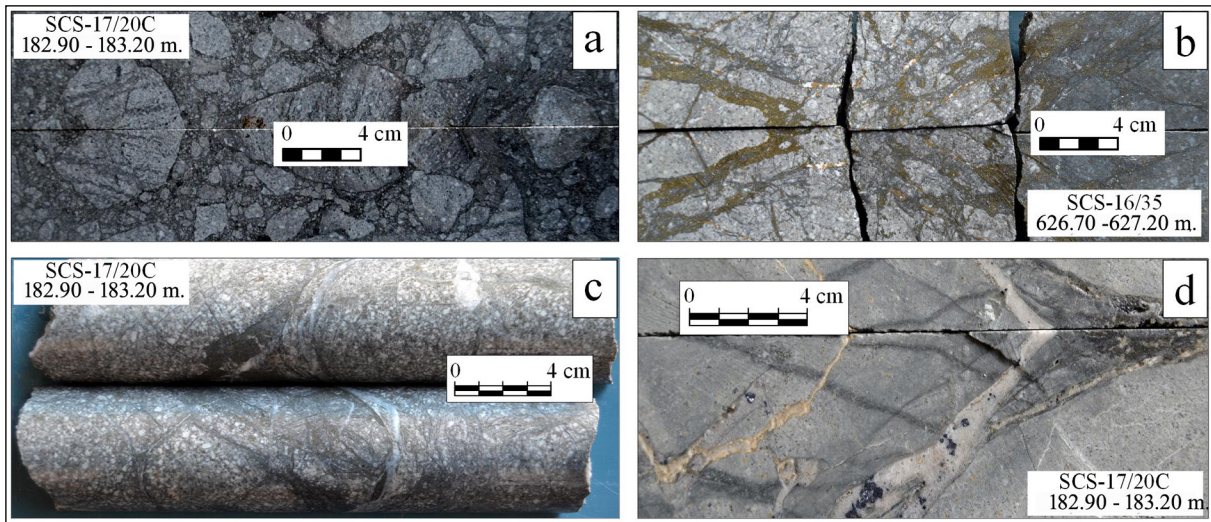


Figure 15- a, b) Disseminated, stockwork brecciated and disseminated quartz veins containing disseminated and pyrite+chalcopyrite+fahlerz group minerals+galena and locally molybdenite in vein-veinlets formed in altered diorite porphyry, c, d) disseminated, stockwork, and brecciated pyrite+chalcopyrite+fahlerz+galena-bearing quartz vein-veinlets with local molybdenite and crosscutting disseminated pyrite+chalcopyrite+galena+sphalerite+gold-bearing barite+quartz+calcite vein-veinlets in altered diorite porphyry are seen.

Type 4 mineralization: They are associated with dense, stockwork white-colored galena+sphalerite+chalcopyrite+gold-bearing barite+quartz+calcite veins-veinlets, which cut the porphyry type Au-Cu deposit.

The mineral assemblages of each mineralization are similar to each other, and the ore microscopy investigation was carried out on a sample with disseminated galena+sphalerite+pyrite and locally chalcopyrite barite+quartz+calcite+dolomite veins formed in diorite porphyry (Figure 16a). Plenty of sphalerite, lesser amount of galena, very little amount of pyrite, traces of chalcopyrite, native gold, fahlerz, and hematite were determined in the sample (Figure 16b-g). Pyrites can be seen as form the main component as coarse crystals in some samples (Figure 16c), sometimes in the form of very fine crystalline fillings in the cracks of sphalerites (Figure 16f), and sometimes as euhedral-subhedral coarse crystals (Figure 16g). Chalcopyrite is observed in the cracks of galena and sphalerite or accompanied by galena and sphalerite (Figure 16b). Chalcopyrite can be seen from place to place as inclusions in pyrite and sphalerite (Figure 16c, g). Native gold is observed in the densely silicified zone, interlocked with and in galena, at the edge, in the cracks and inside of sphalerite with pyrite and in very small and tiny cracks in the densely silicified zone (Figure 16b-g).

6. Fluid Inclusions

6.1. Fluid Inclusion Petrography

Fluid inclusion petrography investigation was carried out on samples from the epithermal (argillic) alteration zone (Figure 17a, b) and porphyry (potassic-phyllitic) alteration zone (Figure 17c, d) selected from BSS-16-11A drill cores. Fluid inclusions in the petrographic investigation of double-polished sections were classified as based on Roedder (1984), Shepherd et al. (1985), and Goldstein and Reynolds (1994). Primary and secondary inclusions, ranging in size from 4-20 μm , are observed in quartz and barite minerals. Inclusions based on the amount and type of components they contain at room temperature are classified as; 1) single-phase (Type I): liquid (L) or vapor (V); 2) two-phase (Type II): liquid-rich (L+V) or vapor-rich (V+L) and 3) multi-phase (Type III): solid phase (mostly salt crystal and opaque mineral) assemblages (Figure 18a-k).

Single-phase, Type I inclusions are 3-10 μm in size, and gas (V) inclusions are more common (Figure 18c). Two-phase, Type II inclusions are 2-20 μm in size and are commonly observed in all zones (Figure 18a, b). Multiphase, Type III inclusions are mostly observed in the potassic zone and it was determined that the inclusions contain more than one solid phase (Figure 18d, e). It has been observed that the liquid,

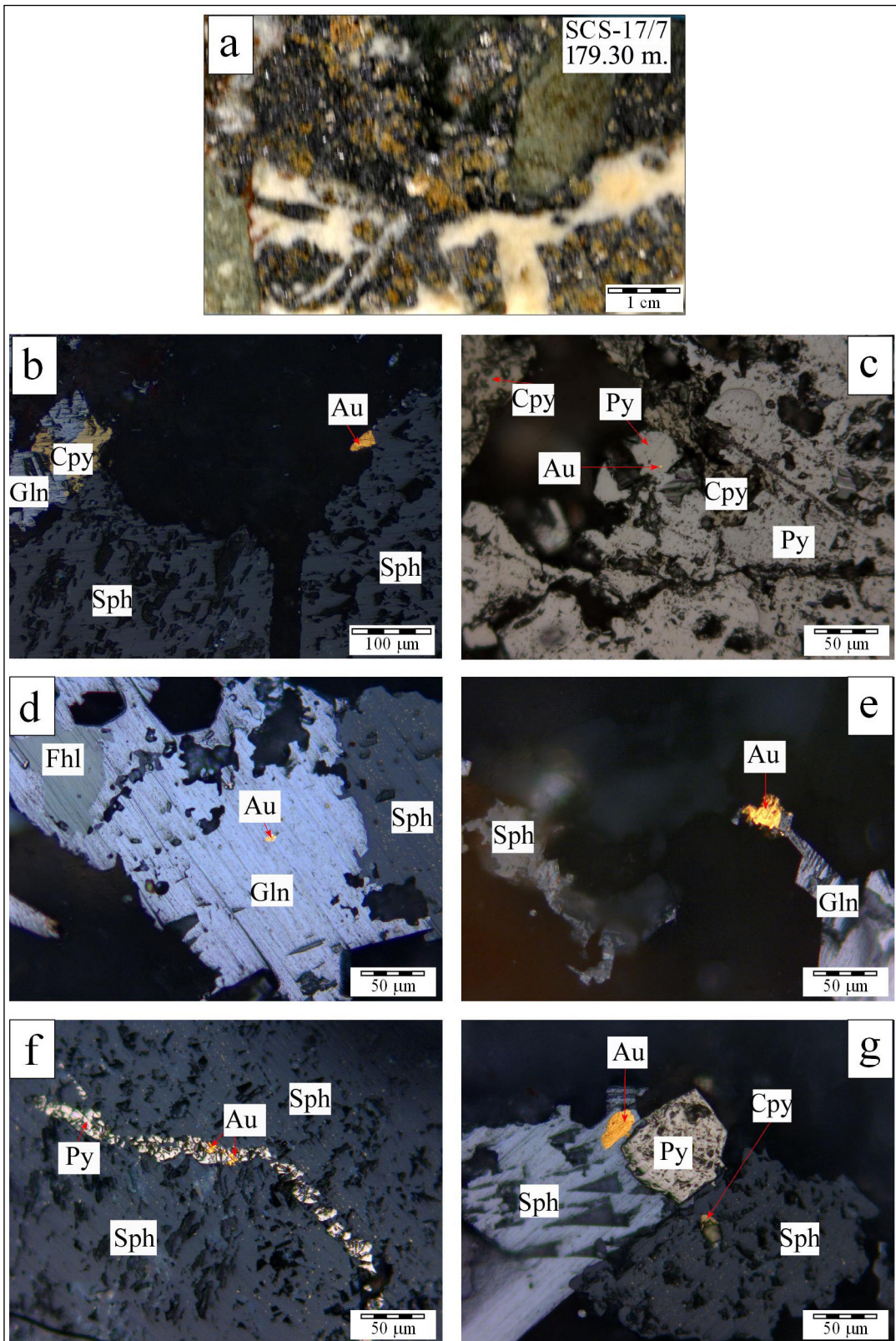


Figure 16- a) Macroscopic view of the zone with abundantly disseminated galena+sphalerite+pyrite, locally chalcopyrite, barite+quartz+calcite veins-veinlets, b) appearance of galena (Gln), sphalerite (Sph), pyrite (Py), chalcopyrite (Cpy), and sphalerite accompanied native gold, c) native gold accumulations with pyrite, chalcopyrite and disseminated pyrite in the intensely silicified zone, d) galena, sphalerite, fahlerz minerals and the formation of native gold in galena, e) galena, sphalerite, fahlerz minerals and the formation of native gold in galena, and f) formation of native gold together with pyrite (Py) in the crack of sphalerite and galena.

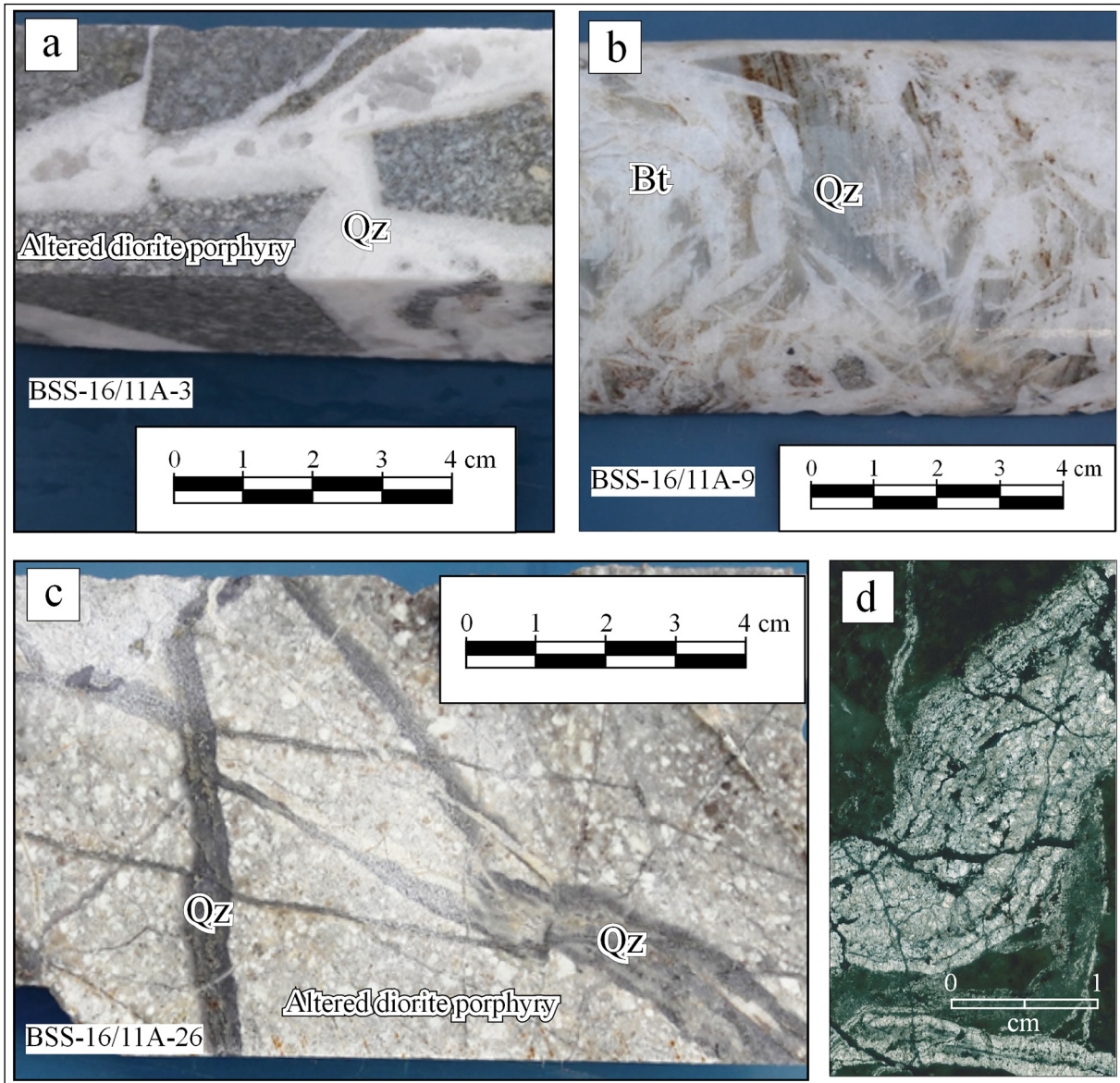


Figure 17- Images of; a) pure quartz (Qz) vein representing the epithermal system, b) quartz (Qz)+barite (Bt) veins, c) undulated quartz veins representing the porphyry system, and d) thin-section scan view from the sample taken from the drill hole BSS-16/11A of Çatalçam mineralization.

vapor, and solid-phase ratios of Type III inclusions are highly variable. Among the minerals observed in Type III inclusions, those with cubic crystal form identified as halite, while opaque minerals with a size of 1-15 μm and red-orange colors are hematite, and those with triangular crystal form identified as chalcopyrite that frequently abundant in fluids of porphyry deposits (Figure 18f, g, and h). The salinity of Type II inclusions is calculated depending on the final ice melting temperature ($T_{m_{ICE}}$), while the salinity of Type III inclusions is calculated based on

the melting point of the halite crystal (Steele MacInnis et al., 2012).

6.2. Micro-thermometric Studies

Micro-thermometric studies were carried out in the inclusions of the samples from the potassic, phyllic and argillic zones. In two-phase inclusions, Type II, TFM values ranging from $-40\text{ }^{\circ}\text{C}$ to $-60\text{ }^{\circ}\text{C}$ were measured. These measured temperature values, when compared with the eutectic temperatures of various water-salt systems, indicate that in addition to NaCl, salts such as

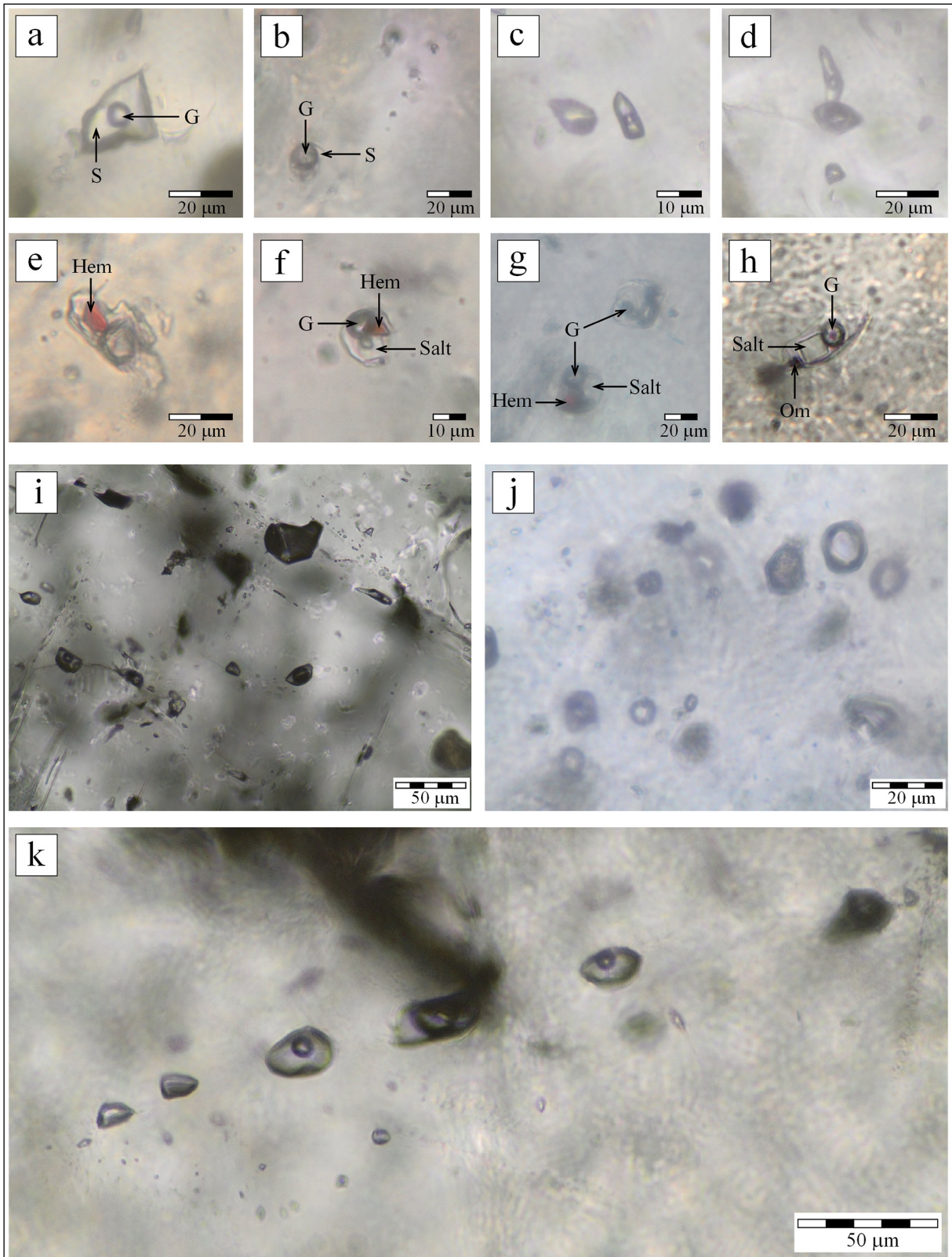


Figure 18- Different types of inclusions indicated in quartz and barite minerals in Çatalçam mineralization. Photomicrographs of; a), b) two-phase inclusions, c) single-phase inclusions, d) vapor-rich two-phase inclusions, e) multiphase inclusions containing hematite, f), g), h) multiphase inclusions containing both hematite and salt and opaque mineral (chalcopyrite?) i) two-component assemblages of inclusions rich in liquid and vapor (FIA), j) low-density vapor-rich inclusions (FIA), k) single- and two-phase inclusion assemblages (FIA).

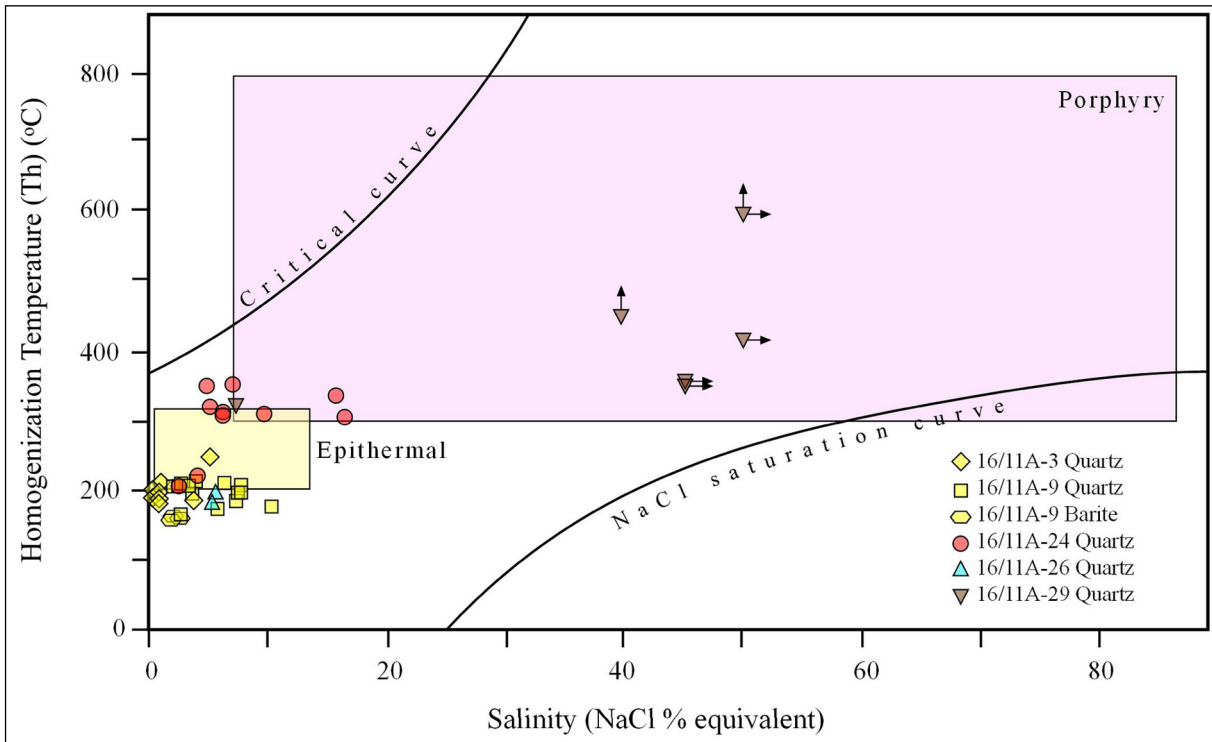


Figure 20- The distribution of salinity versus the homogenization temperature obtained from the fluid inclusions of the Çatalçam mineralization within the porphyry and epithermal types are indicated (Wilkinson, 2001).

respectively. Halılağa, Ağıdağı (Etili, Çanakkale) and Karaayı (Kuşçayır, Çanakkale) porphyry deposits are newly discovered ore deposits (Kuşcu et al., 2019a, b). Other occurrences, for example: Gürcüler, Alaçam, Dikmen, Sarıçayırıyayla, Karapınar, Geleliç, Topuk (Bursa), Tüfekçikonak (Kütahya), Tepeköy (Gökçeada) and Kocatarla (Çanakkale), Eğmir (Edremit) have been extensively explored and drilled with surface and geophysical methods, but there is no information could be found since they have not been publicly announced. In this respect, the Çatalçam mineralization is the most recent example of the porphyry gold deposit discovered in the Biga porphyry belt of the Western Anatolia, and is likely to be the most important considering its lateral and vertical continuation.

The magmatism associated with the mineralizations in the Biga porphyry belt is of Eocene aged lava and lava-dom complexes (49.3-34.3 Ma), pyroclastic rocks, ignimbrite, volcanic breccia andesite, dacite, and locally basalt in the composition (Ercaan et al., 1995; Aldanmaz et al., 2000) and Oligocene andesite, dacite and rhyolite lavas, lithic-crystalline tuff is intercalated or laterally transitional with polymictic

volcanic breccia and conglomerate (Bozkaya and Gökçe, 2001; Bozkaya et al., 2020). Kartaldağ and Serçeler located in the south of Çanakkale, and Ağıdağı and Kirazlı high-sulfidation epithermal deposits located in the west of Çan, are associated with volcanic-plutonic rocks (İmer et al., 2013; Brunetti et al., 2016). Volcanic rocks are generally cut by late Oligocene plutonic rocks (Yiğit, 2012; Bozkaya et al., 2016). Oligocene-Miocene magmatism (30-18 Ma) and related hydrothermal systems (27.4-24.8 Ma) are located in the Biga porphyry belt and are less common in other parts of Turkey. On the other hand, Mid-late Miocene magmatism (about 16-8 Ma) and related porphyry Cu systems are dominant in the Afyon-Konya porphyry belt in Western Anatolia, and it contains the youngest porphyry-related magmatic and hydrothermal systems (14.4-8.9 Ma) (Kuşcu, 2019a).

Çatalçam Au-Pb-Zn-Cu mineralization is a deposit developed within the volcanic-sedimentary rocks of Early Miocene aged with dioritic subvolcanics, which were determined for the first time in the Western Anatolia by the exploration project was conducted between 2011-2017. Field observations and mineralogical-petrographic studies have

shown that potassic, propylitic, phyllic, and argillic alteration zones have developed. These intersecting zones are; from outside to inside: 1) propylitic zone containing epidote, chlorite, calcite, and limonite-hematite with quartz vein-veinlets, altered with pyrite, locally calcite and/or dolomite vein-veinlets that not ore-bearing, 2) argillic zone containing densely clayey, pyrite±chalcopyrite quartz and disseminated galena+sphalerite+chalcopyrite-bearing barite + quartz + calcite + dolomite vein-veinlets (Figures 7 and 21). In the argillic zone, intense sericite, locally clayey (kaolinite), dark gray colored disseminated pyrite±chalcopyrite quartz and galena+sphalerite+chalcopyrite-bearing barite+quartz+calcite+dolomite vein-veinlets and disseminated pyrite phyllic zone were determined. On the other hand, the potassic zone is not observed on the surface, but determined from the drilling cores, in the inner parts of the diorite porphyry, it contains undulated quartz, disseminated galena+sphalerite+chalcopyrite-bearing barite+quartz+calcite+dolomite vein-

veinlets, sericite, and chlorite as well as fine-grained hydrothermal biotite occurrences.

A representative model of the mineralization-associated porphyry system is given in Figure 21. Along the tectonic zones developed within the porphyry type Au-Cu mineralization with disseminated chalcopyrite+gold-bearing quartz veins and chalcopyrite, meteoric waters moved downwards, were heated, and moved towards the surface as hydrothermal fluid. During its upward movement, it dissolved the low-grade gold formed in the porphyry system and absorbed and re-precipitated it together with Zn+Pb+Au+Cu in the stockwork barite+quartz+calcite+dolomite veins. Au with an average grade of about 0.25 gr/ton in the porphyry system, is enriched up to 55 gr/ton from place to place in the epithermal system. Zones with an average of 1 gr/ton Au between 0-220 m and 300-500 m were formed, with less than 1 gr/ton at 220-300 m. Due to the hydrothermal fluids

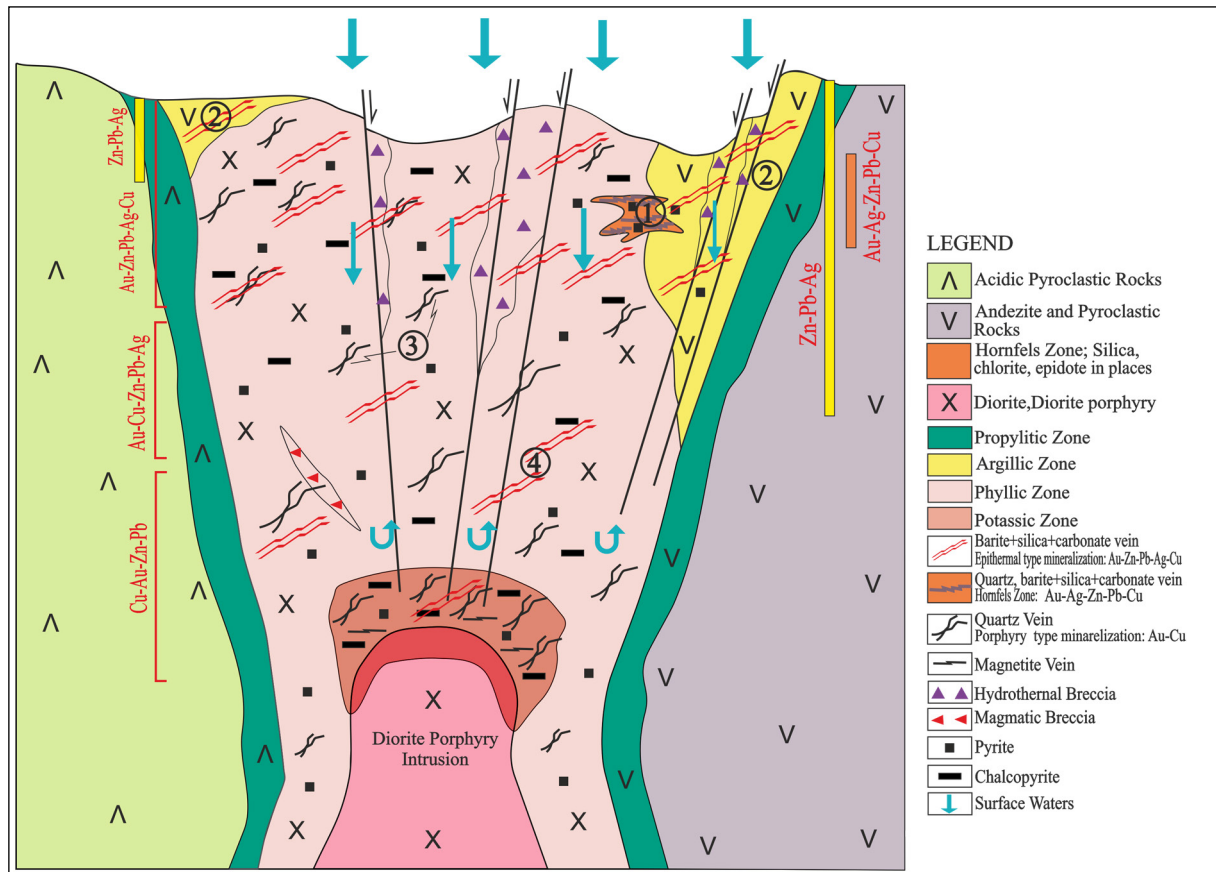


Figure 21- Representative model of the porphyry system of the Çatalçam mineralization and the vertical and lateral distributions of ore-bearing zones and alteration zones (1: ore-bearing quartz in Hornfels, 2: ore-bearing barite-quartz, calcite and/or dolomite in andesites, 3: ore-bearing quartz in Çatalçam Pluton, 4: ore-bearing barite-quartz in diorite porphyry and calcite and/or dolomite).

moving upwards without reaching the porphyry type mineralization, the stockwork disseminated lead+zinc-bearing barite+quartz+calcite+dolomite vein-veinlets in the epithermal system do not contain gold but only silver. Since the epithermal system largely masks the porphyry system; in the phyllic zone, quartz vein-veinlets belonging to the porphyry system are observed as cut and fragmented by barite+quartz+calcite+dolomite vein-veinlets of different sizes. Barite+quartz+calcite+dolomite veins belonging to the epithermal system are also occasionally seen in the potassic zone.

The Cu-Zn-Au-Mo and Sb-As-Ag-Pb-Zn-Cu-Au anomaly groups previously established by the MTA team in the field (Sarı et al., 2018a, b), reveal the Early Miocene aged Yürekli dacite and Yuntdağ volcanics and it overlaps with the alteration areas developed due to the Çatalçam Pluton intruded to the Soma formation. In the Çatalçam Pluton, which is the source of the mineralization, disseminated sulfide, sulphosalts minerals (pyrite, chalcopyrite, galenite, fahlerz), native gold and molybdenite minerals were determined in gray, dark gray colored, locally stockwork-brecciated quartz veinlets. Intense, stockwork white-colored galena+sphalerite+chalcopyrite+gold-bearing barite+quartz+calcite+dolomite veins-veinlets, which cut the porphyry type gold+copper mineralization developed in the diorite porphyry body.

Fluid inclusion assemblages (high homogenization temperature and salinity, abundance of opaque minerals such as hematite and chalcopyrite, and inclusion assemblages of different densities and existence of all these inclusions) determined in the quartz minerals belong to the veins of Çatalçam mineralization show characteristic of porphyry type deposits. Data indicating an epithermal system overlying the porphyry system (lower homogenization temperature and salinity) were also determined by petrographic and micro-thermometric studies.

Textural, optical, and ore microscopy, XRD mineralogy, and fluid inclusion data support the idea that porphyry type Au mineralization and its overprinting epithermal Pb-Zn-Cu-Au mineralization may occur, according to the surface and drilling studies carried out in the field. Oligo-Miocene aged magmatic units have been targeted in metallic mineral exploration projects carried out in Western Anatolia and the Biga Peninsula. However, as a result of this

study, it is seen that not only the Oligo-Miocene aged units but also cutting younger magmatic units may have ore carrier and/or forming characteristics.

Acknowledgements

This study is based on the data obtained from the exploration project 'Polymetallic Mineral Explorations in the Biga Peninsula and the South' conducted by the General Directorate of Mineral Research and Exploration Department (MTA). We would like to thank the Mineral Research and Exploration Department and MTA Northwest Anatolia Regional Directorate for their contribution during the project. We are most grateful to Geology Engineer Esra OKUR and Geology Engineer Beyit YILMAZ who work for Department of Mineral Analysis and Technology and carried out the mineralogical-petrographic analysis. We would like to thank the staff of the MTA Department of Feasibility Studies. We also would like to thank Prof. Dr. Ahmet GÖKÇE (Cumhuriyet University), Prof. Dr. Emin ÇİFTÇİ (Istanbul Technical University), and the anonymous reviewer for their constructive revisions and comments on the manuscript.

References

- Akyürek, B., Sosyal, Y. 1978. Kırkağaç - Soma (Manisa) Savaştepe - Korucu - Ayvalık (Balıkesir), Bergama (İzmir) civarının jeolojisi. Maden Tetkik ve Arama Genel Müdürlüğü, Rapor No: 6452, Ankara (unpublished).
- Akyürek, B., Sosyal, Y. 1983. Biga yarımadası güneyinin (Savaştepe - Kırkağaç - Bergama - Ayvalık) temel jeoloji özellikleri. Bulletin of the Mineral Research and Exploration 95(96), 1-12.
- Aldanmaz, E., Pearce, J. A., Thirlwall, M. F., Mitchell, J. G. 2000. Petrogenetic evolution of Late Cenozoic, post-collision volcanism in western Anatolia, Turkey. Journal of Volcanology and Geothermal Research 102, 67-95.
- Altunkaynak, Ş., Genç, Ş. G. 2008. Petrogenesis and time-progressive evolution of the Cenozoic continental volcanism in the Biga Peninsula, NW Anatolia (Turkey). Lithos 102, 316-340.
- Benda, L., Innocenti, F., Mazzuoli, R., Radicati, F., Steffens, P. 1974. Stratigraphic and radiometric data of the Neogene in northwest Turkey. Zeitschrift der deutschen geologischen Gesellschaft 125, 183-193.

- Bodnar, R. J. 1993. Revised equation and table for determining the freezing point depression of H₂O - NaCl solutions. *Geochimica Cosmochimica Acta* 57, 683-684.
- Borsi, S., Ferrara, G., Innocenti, F., Mazzuoli, R. 1972. Geochronology and petrology of recent volcanics in the eastern Aegean. *Bulletin Volcanologique* 36, 473-496.
- Bozkaya, G., Gökçe, A. 2001. Koru (Çanakkale) Pb - Zn yataklarının jeolojisi, cevher mikroskopisi ve sıvı kapanım özellikleri. *Cumhuriyet Üniversitesi Mühendislik Fakültesi Dergisi, Seri A-Yerbilimleri* 18 (1), 55-70.
- Bozkaya, Ö., Bozkaya, G., Uysal, I. T., Banks, D. 2016. Illite occurrences related to volcanic hosted hydrothermal mineralization in the Biga Peninsula NW Turkey: Implications for the age and origin of fluids. *Ore Geology Reviews* 76, 35-51.
- Bozkaya, G., Bozkaya, Ö., Banks, D. A., Gökçe, A. 2020. P - T - X constraints on the Koru epithermal base - metal (\pm Au) deposit, Biga Peninsula, NW Turkey. *Ore Geology Reviews* 119, 103349.
- Brunetti, P., Miškovic, Hart, C. J. R., Davies, A., Creaser, R. 2016. Geology of the Halilağa porphyry Cu - Au deposit and emergence of an Eocene porphyry Cu belt in NW Turkey. *Society of Economic Geologists - MJD Conference 2016, Çeşme, Turkey*.
- Chen, J., Xu, J., Wang, B., Yang, Z., Ren, J., Yu, H., Liu, H., Fen, Y. 2015. Geochemical differences between subduction - and collision-related copper-bearing porphyries and implications for metallogenesis. *Ore Geology Reviews* 70, 424-437.
- Dönmez, M., Türkecan, A., Akçay, A. E., Hakyemez, Y., Sevin, D. 1998. İzmir ve Kuzeyinin jeolojisi Tersiyer volkanizmasının petrografik ve kimyasal özellikleri. *Maden Tetkik ve Arama Genel Müdürlüğü, Rapor No: 10181, Ankara (unpublished)*.
- Duru, M., Dönmez, M., Ilgar, A., Pehlivan, Ş., Akçay, A. E. 2012. Biga Yarımadası'nın Genel ve Ekonomik Jeolojisi. Editörler: Erdoğan Yüzer ve Gürkan Tunay. *Maden Tetkik ve Arama Genel Müdürlüğü, Özel Yayın Serisi* 28, 326.
- Ercan, T., Günay, E., Savaşçın, Y. 1984. Simav ve çevresindeki Senozoyik yaşlı volkanizmanın bölgesel yorumlanması. *Bulletin of the Mineral Research and Exploration* 97(98), 86-101.
- Ercan, T., Satır, M., Steinitz, G., Dora, A., Sarıfakıoğlu, E., Adis, C., Walter, H. J., Yıldırım, T. 1995. Biga Yarımadası ile Gökçeada Bozcaada ve Tavşan adalarındaki (KB Anadolu) Tersiyer volkanizmasının özellikleri. *Bulletin of the Mineral Research and Exploration* 117, 55-86.
- Ercan, T., Satır, M., Sevin, D., Türkecan, A. 1996. Batı Anadolu'daki Tersiyer ve Kuvaterner yaşlı volkanik kayalarda yeni yapılan radyometrik yaş ölçümlerinin yorumu. *Bulletin of the Mineral Research and Exploration* 119, 103-112.
- Genç, Ş. C., Dönmez, M., Akçay, A. E., Altunkaynak, Ş., Eyüpoğlu, M., Ilgar, Y., 2012. Biga yarımadası Tersiyer volkanizmasının stratigrafik, petrografik ve kimyasal özellikleri. *Biga Yarımadası'nın Genel ve Ekonomik Jeolojisi, MTA Özel Yayın Serisi* 28, 122-162.
- Goldstein, R. H., Reynolds, T. J. 1994. Systematics of fluid inclusions in diagenetic minerals. *Society of Economic Paleontologists and Mineralogists Short Course*, Tulsa, 199.
- Hou, Z., Zhang, H., Pan, X., Yang, Z. 2011. Porphyry (Cu - Mo -Au) deposits related to melting of thickened mafic lower crust: examples from the eastern Tethyan metallogenic domain. *Ore Geology Reviews* 39, 21-45.
- İmer, E. Ü., Güleç, N., Kuşcu, İ., Fallick, A. E. 2013. Genetic investigation and comparison of Kartaldağ and Madendağ epithermal gold deposits in Çanakkale NW Turkey. *Ore Geology Reviews* 53, 204-222.
- İnci, U. 1998. Miocene synvolcanic alluvial sedimentation in lignite-bearing Soma Basin, Western Turkey. *Turkish Journal of Earth Sciences* 7(2), 63-78.
- İnci, U. 2002. Depositional evolution of Miocene coal successions in the Soma coalfield, western Turkey. *International Journal of Coal Geology* 51, 1-29.
- Janković, S. 1997. The Carpatho-Balkanides and adjacent area: a sector of the Tethyan Eurasian metallogenic belt. *Mineralium Deposita* 32, 426-433.
- Jingwen, M., Pirajno, F., Lehmann, B., Maocheng, L., Berzina, A. 2014. Distribution of porphyry deposits in the Eurasian continent and their corresponding tectonic settings. *Journal of Asian Earth Sciences* 79, 576-584.
- Karaoğlu, Ö. 2014. Tectonic controls on the Yamanlar volcano and Yuntdağı volcanic region, western Turkey: implications for an incremental deformation. *Journal of Volcanology and Geothermal Research* 274, 16-33.
- Ketin, İ. 1966. Anadolu'nun tektonik birlikleri. *Bulletin of the Mineral Research and Exploration* 66, 23-34.

- Konak, N. 2002. 1/500.000 Türkiye Jeoloji Haritası İzmir Paftası. Maden Tetkik ve Arama Genel Müdürlüğü, Ankara.
- Krushensky, R. D. 1976. Neogene Calc-alkaline extrusive and intrusive rocks of the Karalar Yeşiller area, Northwest Anatolia, Turkey. *Bulletin Volcanologique* 40, 336-360
- Kuşcu, İ., Tosdal, R. M., Gencalioglu Kuşcu, G. 2019a. Episodic porphyry (Cu-Mo-Au) formation and associated magmatic evolution in Turkish Tethyan collage. *Ore Geology Reviews* 107, 119-154.
- Kuşcu, İ., Tosdal, R.M., Gencalioglu Kuşcu, G. 2019b. Porphyry - Cu Deposits of Turkey. Pirajno F., Ünlü, T., Dönmez, C., Şahin, M. (Ed.). *Mineral Resources of Turkey. Modern Approaches in Solid Earth Sciences*. Springer 337-425.
- Li, Y., Selby, D., Condon, D., Tapster, S. 2017. Cyclic magmatic - hydrothermal evolution in porphyry systems: high - precision U-Pb and Re-Os geochronology constraints on the Tibetan Qulong porphyry Cu - Mo deposit. *Economic Geology* 112, 1419-1440.
- Lu, Y. J., Loucks, R. R., Fiorentini, M. L., Yang, Z. M., Hou, Z. Q. 2015. Fluid flux melting generated postcollisional high Sr/Y copper ore-forming water-rich magmas in Tibet. *Geology* 43, 583-586.
- Nebert, K. 1978. Linyit ihtiva eden Deniz Neojen sahasının (Soma - Manisa) jeolojisi ve linyit yatakları hakkında rapor. Maden Tetkik ve Arama Genel Müdürlüğü, Rapor No: 2948 (unpublished).
- Okay, A. I., Tüysüz, O. 1999. Tethyan sutures of northern Turkey. Durant, B., Jolivet, F., Horvath, F., Seranne, M. (Ed.). *The Mediterranean basin: Tertiary extension within the Alpine orogen*. Geological Society of London. Special Publication 156, 475-515.
- Oyman, T. 2019. Epithermal Deposits of Turkey. Pirajno F., Ünlü T., Dönmez C., Şahin M. (Ed.). *Mineral Resources of Turkey. Modern Approaches in Solid Earth Sciences*, Springer, 16, 337-425.
- Richards, J. P. 2009. Post - subduction porphyry Cu - Au and epithermal Au deposits: products of remelting of subduction -modified lithosphere. *Geology* 37, 247-250.
- Richards, J. P. 2015. Tectonic, magmatic, and metallogenic evolution of the Tethyan orogen from subduction to collision. *Ore Geology Reviews* 70, 323-345.
- Roedder, E. 1984. Fluid inclusions. *Mineralogical Society of America, Reviews in Mineralogy* 12, 644.
- Saatci, E. S., Aslan, Z. 2018. Petrography and petrology of the Yürekli (Balıkesir) volcanics: an example of post-collisional felsic volcanism in the Biga Peninsula (NW Turkey). *Bulletin of the Mineral Research and Exploration* 157, 103-120.
- Sarı, R., Küçükefe, Ş., Çetiner, L. 2018a. Ar-201300664 no'lu Çatalçam porfiri altın - gümüş - kurşun - çinko sahası (Manisa - Soma - Kiraz ruhsatı) buluculuk talebine esas maden jeolojisi ve kaynak tahmin raporu. Maden Tetkik ve Arama Genel Müdürlüğü, Ankara (unpublished).
- Sarı, R., Küçükefe, Ş., Özkümüş, S., Dönmez, C., Metin, S., Baran, C., Özerkan, Ö., Avşar, M. 2018b. Çatalçam (Soma - Manisa) Au - Pb - Zn - Cu cevherleşmesinde toprak jeokimyası çalışmaları. 8. Jeokimya Sempozyumu, 2 - 6 Mayıs 2018, Antalya, 242-243.
- Shepherd, T. J., Rankin, A. H., Alderton, D. H. M. 1985. *A Practical Guide to Fluid Inclusion Studies*. Blackie, London, UK, 235.
- Steele MacInnis, M., Lecumberri Sanchez, P., Bodnar, R. J. 2012. HokieFlincs H₂O - NaCl: a Microsoft Excel spreadsheet for interpreting microthermometric data from fluid inclusions based on the PVTX properties of H₂O - NaCl, *Computer Geosciences* 49, 334-337.
- Tang, J., Yang, H., Song, Y., Wang, L., Liu, Z., Li, B., Lin, B., Peng, B., Wang, G., Zeng, Q., Wang, Q., Chen, W., Wang, N., Li, Z., Li, Y., Li, Y., Li, H., Lei, C. 2021. The copper polymetallic deposits and resource potential in the Tibet Plateau, China *Geology* 4, 1-16.
- Tetiker, S., Yalçın, H., Bozkaya, Ö., Göncüoğlu M. C. 2015. Metamorphic evolution of the Karakaya Complex in northern Turkey based on phyllosilicate mineralogy. *Mineralogy and Petrology* 109, 201-215.
- Wilkinson, J. J. 2001. Fluid inclusions in hydrothermal ore deposits. *Lithos* 55, 229-272.
- Yalçın, H., Bozkaya, Ö. 2002. Hekimhan Malatya çevresindeki Üst Kretase yaşlı volkaniklerin alterasyon mineralojisi ve jeokimyası: Denizsuyu kayaç etkilesimine bir örnek. *Cumhuriyet Üniversitesi Mühendislik Fakültesi Dergisi Yer Bilimleri* 19, 81-98.
- Yılmaz, Y., Genç, Ş. C., Karacık, Z., Altunkaynak, Ş. 2001. Two contrasting magmatic associations of NW Anatolia and their tectonic significance. *Journal of Geodynamics* 31, 243-271.

Yiğit, Ö. 2009. Mineral deposits of Turkey in relation to Tetyhan metallogeny: implications for future mineral exploration. *Economic Geology* 104, 19-51.

Yiğit, Ö. 2012. A prospective sector in the Tethyan Metallogenic Belt: geology and geochronology of mineral deposits in the Biga Peninsula, NW Turkey. *Ore Geology Reviews* 46, 118-148.

